






## Liquefaction Potential Evaluation by Deterministic and Probabilistic Approaches

Md Belal Hossain <sup>1\*</sup>, Md Roknuzzaman <sup>1</sup>, Md Mahabub Rahman <sup>1</sup>

<sup>1</sup> Department of Civil Engineering, Hajee Mohammad Danesh Science and Technology University, Dinajpur-5200, Bangladesh.

Received 31 March 2022; Revised 19 June 2022; Accepted 24 June 2022; Published 01 July 2022

### Abstract

Bangladesh is one of the world's most disaster-prone areas. The northwest region of Bangladesh is the most seismically active region. Dinajpur is the district closest to the Himalayan frontal thrust, making it the most vulnerable to earthquake-related liquefaction. Therefore, the in-situ parameters are used to assess the liquefaction susceptibility of the subsurface geology for the Dinajpur district in terms of soil liquefaction safety factor (FS), the liquefaction potential index (LPI), and the liquefaction probability (PL). This study used deterministic and probabilistic techniques to estimate the liquefaction susceptibility of the area based on standard penetration test (SPT) N values. SPT data was collected at 160 different places within the study area. In an earthquake scenario with  $M_w = 6.5$ , liquefaction resistance is evaluated at each location using a 0.20g peak ground acceleration (PGA). The results of the SPT-based liquefaction assessment techniques were found to be considerably different. The soil strata prone to liquefaction in different zones of the city have been determined based on a common comparison. According to deterministic and probabilistic techniques, it has been found that, out of 160 locations, 36 and 50 sites are susceptible to liquefaction. Then, using geospatial techniques (IDW interpolation), hazard maps were created depending on the potential for liquefaction of particular locations. Finally, using an independent secondary dataset, the resulting hazard maps were validated to examine the developed approach. The obtained  $R^2$  values for each regression analysis event were more than 0.79. Therefore, the produced hazard map may be utilized successfully for planning, management, and long-term development of the studied locations.

**Keywords:** Earthquake; Peak Ground Acceleration; Factor of Safety; Liquefaction Hazard Map.

## 1. Introduction

Bangladesh is prone to natural catastrophes because of its geographic position and geological characteristics. The earthquake is one of the world's most devastating natural catastrophes [1]. Bangladesh and its adjacent regions are susceptible to earthquakes because of their closeness to the convergent plate boundary between the Indian and Eurasian plates [2-4]. Major earthquakes in the past have caused significant damage in and around Bangladesh, and devastating moderate-magnitude earthquakes happen every few years [5]. Because of their dense populations, uncontrolled growth, and non-engineered construction practices, these places are seismically risky [6]. In these regions, an earthquake with a large magnitude adjacent to a megacity would cause a serious and severe risk to human life, housing, economic growth, and development [7]. Dinajpur is one of the major districts in North Bengal, and it continues to develop as a result of industry and urbanization [8]. Several infrastructures are being created to accommodate the rising demand. Infrastructure destruction and damage are caused by a variety of geotechnical hazards all over the world. Earthquakes are a serious geotechnical hazard that can induce liquefaction [9].

\* Corresponding author: [mbh.civil@hstu.ac.bd](mailto:mbh.civil@hstu.ac.bd)

 <http://dx.doi.org/10.28991/CEJ-2022-08-07-010>



© 2022 by the authors. Licensee C.E.J, Tehran, Iran. This article is an open access article distributed under the terms and conditions of the Creative Commons Attribution (CC-BY) license (<http://creativecommons.org/licenses/by/4.0/>).

Liquefaction is a physical process that can cause soil to collapse in an earthquake event. The soil's strength is greatly reduced as a result of this occurrence, to the point that it can no longer support structures or remain stable. As a result of this process, the earth's sediments will appear to flow like fluids [10-12]. Soil liquefaction occurs when saturated or partially saturated sandy soils lose their strength because of earthquake shaking, resulting in soil liquid behavior. During this process, the pore water pressure in the soil's core rises, reducing the total effective stress caused by earthquake loading. Effective stress is reduced to a minimum when pore pressure equals total stress, causing soil particles to be suspended in water and liquefaction [13]. According to Seed & Idriss (1967), the devastating occurrence of liquefaction caught the attention of numerous scholars during the 1964 Niigata earthquakes, in which many structures were tilted [14]. In 1999, there was a well-known incident of soil liquefaction that occurred in Adapazar, Turkey. As a result, a significant portion of the city was destroyed, and a huge number of people died. During this earthquake, liquefaction of the soil was detected [15]. According to Bray & Sancio (2006), the 1999 earthquake in the Adapazar area caused fine-grained soils (clay and silt) to liquefy at 12 construction sites [16]. Due to the possibility of earthquakes, researchers conducted a few investigations in and around Bangladesh to estimate liquefaction probability at the local level.

Ansary and Rashid [17] conducted a case study in 2000 using data from 190 bore holes from the Standard Penetration Test to assess the Greater Dhaka Metropolitan Area, Bangladesh's vulnerability to liquefaction. A liquefaction vulnerability map was created after the liquefaction potential was assessed using two simplified approaches. Based on the findings of standard penetration tests, Islam and Ahmed performed an investigation in 2010 to evaluate the liquefaction potential of a few specified reclaimed areas of Dhaka city. It was observed that some areas of the reclaimed areas are liquefiable up to the filling depth [18]. In 2010, Mhaske and Choudhury carried out research to create a map of Mumbai's overall sensitivity to soil liquefaction by defining three zones: critically liquefiable soil; moderately liquefiable soil and non-liquefiable soil. The assessment of the factor of safety against soil liquefaction potential was done using a simplified version of the Youd et al. (2001) approach. It was reported that locations such as Borivali, Malad, Dahisar, and Bhandup are susceptible to liquefaction for earthquakes of moment magnitudes of  $M_w = 5.0$  and  $7.5$  [19]. Shukla et al. (2013) performed a study to assess the liquefiable underlying soil in a portion of Delhi University North Campus because the city continues to develop high-rise buildings and other mega structures despite having a good number superstructure already. The analysis of the study found that the average depth of subsurface soil that is liquefiable in the study region is greater than 8 meters. The study's final finding was that the region is extremely vulnerable to earthquake liquefaction and needs the proper mitigation to lower down the risk [20]. Hossain et al. (2020) conducted a recent case study in which they used a standard penetration test data to estimate the liquefaction potential index for a small town (Moulvibazar) in northeast Bangladesh. The LPI values for each borehole's soil profile were derived using the 25 bore log SPT-N data with an earthquake magnitude of  $M_w=8$  and a peak horizontal ground acceleration (PGA) of  $0.36$  g. The LPI values in town range from 0 to 42.33, with values ranging from 1.42 to 7.52 in the Holo-Pleistocene zone and 0 to 42.34 in the Holocene flood plain area [21].

Sengupta and Kolathayar (2020) performed another case study, evaluating the liquefaction potential of a combined-cycle power plant site in Bangladesh's Chittagong area. The liquefaction potential of the site was evaluated using the SPT-N values of 33 boreholes located at 3-meter intervals from the ground level to a depth of 30 meters. Following investigation, researchers indicated that the soil up to 15 meters deep had a considerable liquefaction risk at successive depths in the majority of drilling locations [22]. Using information from 28 boreholes, Wadi et al. (2021) carried out a similar case study at a sugar plant location in Nigeria's Upper Benue area to assess subsurface formation for soil liquefaction analysis. According to the method in Idriss and Boulanger, the liquefaction parameters were calculated (2014). According to the findings, there is saturated loose to medium-density sandy, silty clayey soil between 1.5 and 4.5 meters beneath the surface, and the liquefaction safety factor is less than 1 [23]. The study by Abdullah and Aal (2021) was aimed at assessing and creating maps of Jeddah City's vulnerability to liquefaction in the Kingdom of Saudi Arabia. By using data from 214 SPT boreholes, the liquefaction potential index (LPI) was evaluated. The findings indicate that the majority of the city of Jeddah is located in a region with a relatively low liquefaction potential, with the exception of the sites in the Abhur and Al-Hamra districts, where it is moderate to high [24].

Subedi and Acharya (2022) conducted the most current case study to estimate the liquefaction potential of the Kathmandu valley, Nepal, utilizing borehole data comprising SPT-N values from 410 sites. For the assessments, certain current and widely used analytical and computing methods were applied, and the findings were presented in the form of liquefaction hazard maps. The evaluation results found that the majority of the sites had medium to very high liquefaction susceptibility, with the center and southern sections of the valley being more sensitive to liquefaction and at greater risk of liquefaction damage than the northern parts [25]. According to Tint et al. (2018), Yangon City, Myanmar, was recently hit by several major earthquakes. As a result, the liquefaction potential index (LPI) was estimated using the Luna and Frost Technique in 1998, after computing the safety factor of soil liquefaction using the simplified approach. Finally, maps of liquefaction hazard were created that corresponded to seismicity and had a yearly probability of exceedance values of 1%, 2%, and 10% in 50 years [26]. During the earthquakes in Bengal (1885), in Great India (1897), and in Srimangal (1918), significant liquefaction cases were seen in Bangladesh's alluvial deposits [21]. Pleistocene monoliths and alluvial deposits make up the town's subsurface soils (sand, silt, and clay). Due to its location in an earthquake-

prone area, alluvial soil, and a high groundwater table, this area has a significant potential for liquefaction caused by earthquakes. However, no research has been done to evaluate the liquefaction vulnerability of this region. Therefore, liquefaction hazard evaluation for the city is necessary to secure a reliable urban development. The main objectives of the current study are to determine the soil liquefaction safety factor, the liquefaction potential index (LPI), and the liquefaction probability (PL) for the subsurface geology of the Dinajpur District. This assessment will be conducted using simplified deterministic and probabilistic approaches. In order to calculate the LPI and PL values of the soil profiles, the safety factors against liquefaction for different layers of soil are assessed using an Mw 6.5 earthquake scenario with a PGA value of 0.20g. Finally, geospatial techniques were utilized to create severity maps for the study area. The vulnerable zones were identified using the hazard map.

## 2. Seismotectonics and Surface Geology

Plate tectonics is intimately linked to earthquakes. Bangladesh is positioned near the plate borders of the Indian and Eurasian plates in a tectonically active zone (Figure 1). Bangladesh is located to the north and east of the plate borders. Significant thrust faults may be found in Bangladesh's north (at the base of the Himalayas) and east (in the Indo-Burma mountainous regions) [6]. Dinajpur is the largest of Bangladesh's sixteen northern districts. Dinajpur is the district with the greatest proximity to the mountain frontal thrust.

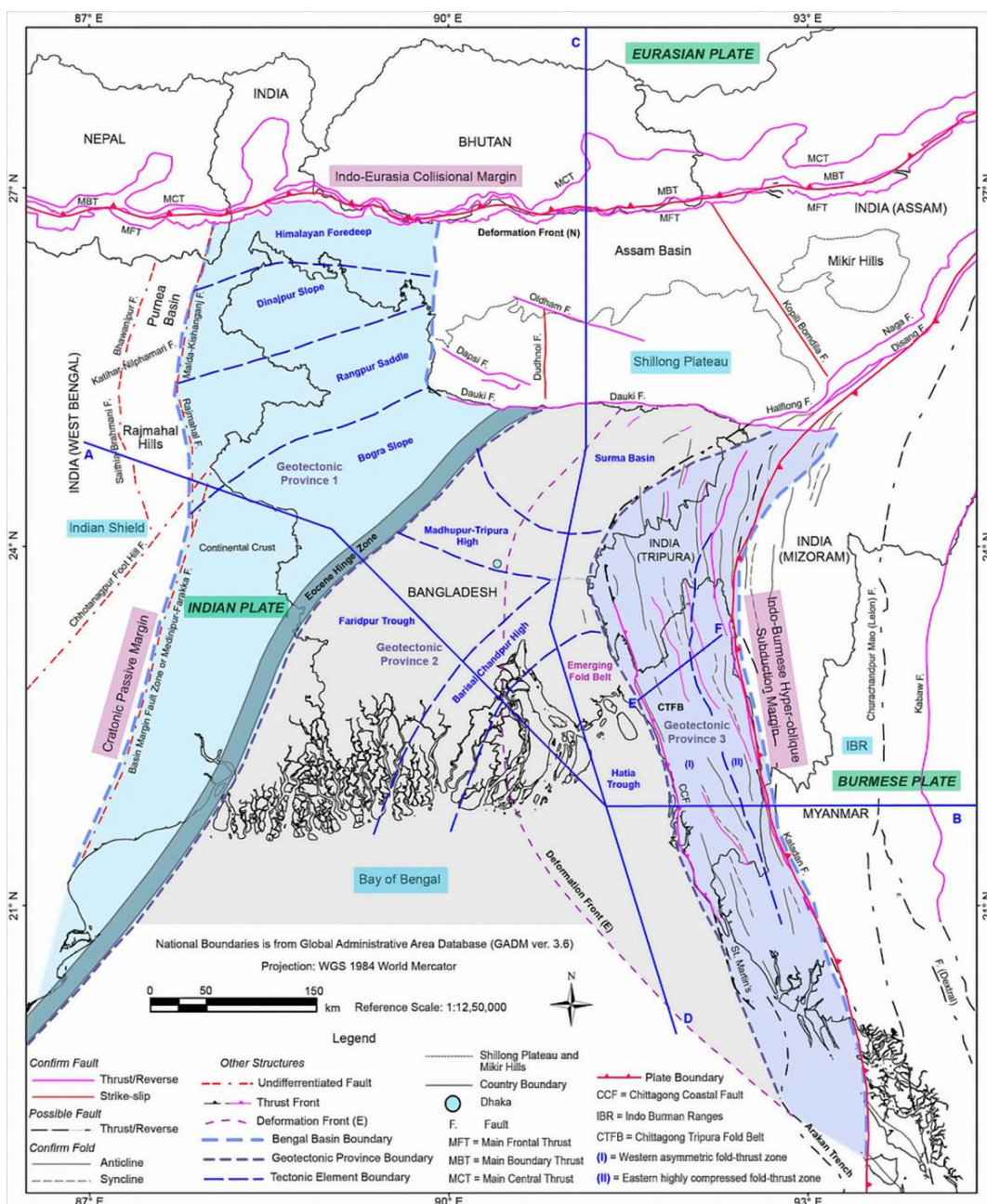


Figure 1. Simplified schematic tectonic map of the Bengal Basin and its surroundings [27] (Adopted from Hossain et al. [28] and Khan et al. [29])

Because the Indian and Eurasian plates collide, the Himalayan Ranges in the north and the Indo–Burman Ranges in the east are produced, and the Bengal Basin is formed in the eastern half of the Indian Plate [30]. The northeast migrating Indian Plate collides with the Eurasian Plate, causing earthquakes in North East India, Bangladesh, Nepal, and Myanmar. Historically, five earthquakes of significant magnitude (M7.0) struck Bangladesh between 1869 and 1930. These earthquakes occurred in 1869 in Cachar, 1885 in Bengal, 1897 in Great India, 1918 in Srimangal, and 1930 in Dhubri. The earthquakes caused damage in Bangladesh's northern, northeastern, southeastern, and central regions [31]. The Great Indian and Dhubri earthquakes have had a significant impact on the northern section of the country. These incidents caused the most damage to railway lines and structures. The incidence and damage caused by several earthquakes (magnitudes ranging from 4 to 6) within the nation or near the country's border have sparked concern in recent years.

Bangladesh's geology is characterized by folded tertiary sedimentary rocks (sandstone, shale, and siltstone) in the southeast and northeast, isolated Pleistocene monoliths (silt, clay, silt, and sand), and alluvial layers (sand, silt, and clay) in the central, northwest, and eastern regions [32]. The study area is located in Bangladesh's northwestern area and is characterized by a mountain frontal thrust (Figure 2).

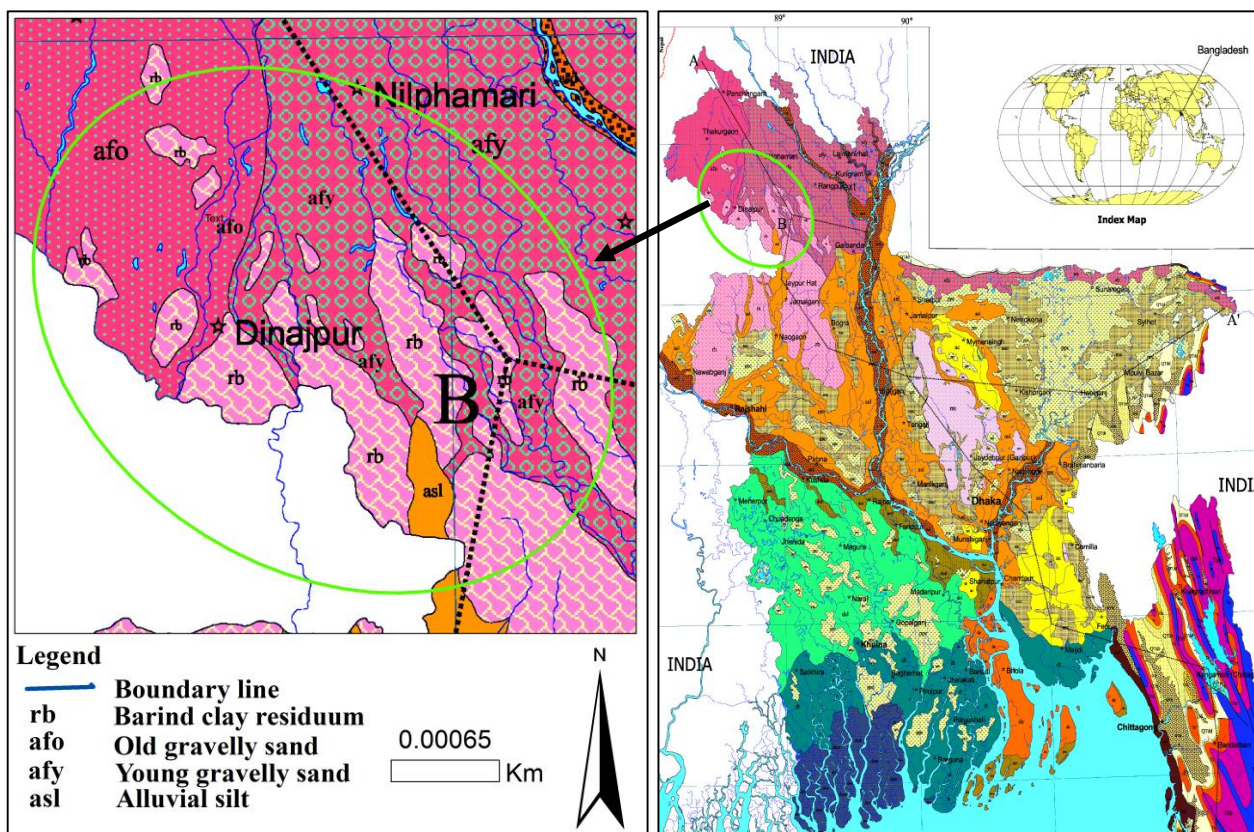


Figure 2. A geological map of the northwest part of Bangladesh. The details are taken from a geological map prepared by Alam et al. [32]

The surface geology of the studied region exhibits four unique patterns. The Barind clay residuum and the old gravelly sand run through the district's northern section. Young gravelly sand covers the northern section of the district. The majority of the region in the south and southeast is covered with Barind clay residuum, along with young gravelly sand and alluvial silt. Because of the city's increasing growth, the risk is becoming more serious. The presence of cohesionless soil at shallow depths over much of the study area increases the risk of liquefaction.

### 3. Methodology

#### 3.1. Deterministic Approaches

In most cases, the Seed and Idriss (1971) technique has proven to be a suitable fit and can be a feasible option for liquefaction assessment among several simpler processes [33, 35]. The Tokimatsu and Yoshimi [34] approach yielded positive outcomes in some cases. The original Seed and Idriss approach has been improved by Idriss and Boulanger [35, 36], which has proven to be effective in practice. As a result, these three deterministic techniques were used to assess the liquefaction susceptibility.

### 3.1.1. Seed's Method

The cyclic stress ratio (CSR), which can be evaluated using the suggested equation, is the denominator component of the liquefaction resistance [35].

$$CSR = 0.65 \times \frac{a_{\max}}{g} \times \frac{\sigma_v}{\sigma_v'} \times r_d \quad (1-a)$$

In Equation 1-a, CSR= cyclic stress ratio,  $a_{\max}$  = highest horizontal ground acceleration due to earthquake,  $g$  = acceleration due to gravity,  $\sigma_v$  = vertical total stress,  $\sigma_v' = (\sigma_v - u)$  = vertical effective total stress,  $u$  = pressure of pore water,  $r_d$  = stress reduction factor.

At the same time, the SPT-N value may be utilized to evaluate the cyclic resistance ratio (CRR). The CRR suggested by Youd et al. [37] may be estimated using the equation below:

$$CRR_{7.5} = \frac{a + cx + ex^2 + gx^3}{1 + bx + dx^2 + fx^3 + hx^4} \quad (1-b)$$

In Equation 1 – b, the terms,  $x = N_{1,60,FC}$ ,  $a = 0.048$ ,  $b = -0.1248$ ,  $c = -4.421 \times 10^{-3}$ ,  $e = 6.13 \times 10^{-4}$ ,  $f = -3.285 \times 10^{-4}$ ,  $g = -1.673 \times 10^{-5}$ ,  $h = 3.714 \times 10^{-6}$ .

### 3.1.2. Tokimatsu and Yoshimi (T-Y) Method

The seismic demand generated by a specific earthquake is described by the cyclic stress ratio (CSR). Tokimatsu and Yoshimi [34] developed the following equation for CSR produced by earthquake ground movements.

$$CSR = 0.1 \times (M - 1) \times \frac{a_{\max}}{g} \times \frac{\sigma_v}{\sigma_v'} \times r_d \quad (2-a)$$

In Equation 2-a, Stress reduction factor,  $r_d = 1 - 0.015z$ ,  $M$  stands for Earthquake Magnitude and other terms explained above.

Tokimatsu and Yoshimi [34] also established the Cyclic Resistance Ratio (CRR):

$$CRR = a \times C_r \left[ \left( \frac{16\sqrt{N_a}}{100} \right) + \left( \frac{16\sqrt{N_a}}{C_s} \right)^n \right] \quad (2-b)$$

where,  $a = 0.45$ ,  $C_r = 0.57$ ,  $n = 14$ ,  $C_s = 80-9$ ,  $C_s = 75$  for extensive liquefaction situation and  $N_a$  in Equation 2-b can be calculated as Tokimatsu and Yoshimi [34].

### 3.1.3. Idriss and Boulanger Method

The following equation gives the cyclic stress ratio (CSR) generated by the design earthquake, as suggested by Idriss and Boulanger [36]:

$$CSR = 0.65 \times \frac{a_{\max}}{g} \times \frac{\sigma_v}{\sigma_v'} \times r_d \quad (3-a)$$

In Equation 3-a, CSR= cyclic stress ratio,  $a_{\max}$  = highest horizontal ground acceleration due to earthquake,  $g$  = acceleration due to gravity,  $\sigma_v$  = vertical total stress,  $\sigma_v' = (\sigma_v - u)$  = vertical effective total stress,  $u$  = pressure of pore water,  $r_d$  = stress reduction factor.

For,  $z \leq 34$  m:

$$r_d = \exp[\alpha(z) + \beta(z)M] \quad (3-b)$$

where  $\alpha(z) = -1.012 - 1.126 \sin\left[\frac{z}{11.73} + 5.133\right]$ ,  $\beta(z) = 0.106 + 0.118 \sin\left[\frac{z}{11.28} + 5.142\right]$ .

For,  $z > 34$  m,

$$r_d = 0.12 \exp(0.22M) \quad (3-c)$$

where,  $z$  is the depth of the earth under the surface in meters and  $M$  represents the earthquake's magnitude. The soil's ability to withstand liquefaction, as determined by the corrected N-value of each soil layer, is known as the cyclic resistance ratio. Rauch [38] found the following equation for calculating  $CRR_{7.5}$ .

$$CRR_{7.5} = \frac{1}{34 - (N_1)_{60}} + \frac{(N_1)_{60}}{135} + \frac{50}{10 \cdot (N_1)_{60}^{0.45}} - \frac{1}{200} \quad (3-d)$$

### 3.1.4. Evaluation of Factor of Safety (FS)

The Factor of Safety is calculated using the following equation for various strata and earthquake magnitudes [35]:

$$F_s(\text{Factor of safety}) = \frac{\text{CRR}_{7.5}}{\text{CSR}} \times \text{MSF} \quad (4)$$

In Equation 4, the cyclic stress ratio is abbreviated as CSR, The cyclic resistance ratio for earthquakes of magnitude 7.5 is known as  $\text{CRR}_{7.5}$  and The MSF stands for magnitude scaling factor.

### 3.1.5. Assessment of Liquefaction Potential Index (LPI)

To estimate local liquefaction potential, the Liquefaction Potential Index (LPI) is a single-valued measure. The safety factor is integrated along with the soil profile to calculate the LPI at a given location. A weighting algorithm has been implemented to provide the layers closest to the earth's surface with greater weight. The Liquefaction Potential Index (LPI) introduced by Luna and Frost [39] can be stated as follows:

$$\text{LPI} = \sum_{i=1}^n w_i F_i H_i \quad (5)$$

Here,  $F_i = 1 - \text{FS}_i$ , for  $\text{FS}_i < 1.0$ ;  $F_i = 0$ , for  $\text{FS}_i \geq 1.0$ ;  $W_i = 10 - 0.5z_i$ , for  $z_i \leq 20\text{m}$ ;  $W_i = 0$ , for  $z_i > 20\text{m}$ .

where,  $n$  specifies the discretized layer number.  $H_i$  is the discretized layer's thickness,  $F_i$  signifies the severity of liquefaction for a layer, which is a function of the FS described in Equation.,  $\text{FS}_i$  denotes safety factor for  $i$ -th layer,  $w_i = 10 - 0.5z_i$ , which denotes weighting factor and  $z_i$  stands for depth of  $i$ -th layer in meter. Therefore, the Liquefaction Potential Index is used to measure the liquefaction hazard. When the LPI surpasses 15.0, the location is considered to be severely liquefied. A LPI of less than 5.0 suggests very little to minor liquefaction severity, whereas an LPI of 5 to 15.0 indicates moderate liquefaction [40].

### 3.1.6. Determination of Magnitude Scaling Factor (MSF)

The magnitude scaling factor (MSF) is used to adapt the induced CSR when an earthquake of any magnitude occurs. Youd and Idriss [41] give a method for calculating magnitude scaling factor.

$$\text{MSF} = \frac{10^{2.24}}{M_w^{0.56}} \quad (6)$$

In Equation 6, earthquake's Richter magnitude is measured in  $M_w$ . The flowchart below illustrates the methodical approach for determining the liquefaction safety factor, liquefaction potential index, and liquefaction probability for the study region (Figure 3).

## 3.2. Probabilistic Approaches

Toprak et al. [42] used logistic regression studies to create SPT-based probabilistic liquefaction boundary curves. The logistic regression formula derived using the new global liquefaction database (total data sets = 440).

$$\text{Logit}(P_L) = \ln \frac{P_L}{1-P_L} = 10.4459 - 0.2295(N_{1,60CS}) + 4.0573 \ln \left( \frac{\text{CSR}}{\text{MSF}} \right) \quad (7)$$

In Equation 7,  $P_L$  = probability of liquefaction.  $\text{CSR}$  = cyclic stress ratio, must be evaluated according to Youd et al. [41]. Using the magnitude scaling factor (MSF), the  $\text{CSR}$  values were modified to  $M_w = 7.5$ .  $N_{1,60CS}$ , the adjusted equivalent clean-sand blow count is calculated according to Youd et al. [41]. Juang et al. [43] used logistic regression as indicated in Equation 8, on a data set of 243 samples with SPT values:

$$\text{Logit}(P_L) = \ln \frac{P_L}{1-P_L} = 10.1129 - 0.25729N_{1,60CS} + 3.4825 \ln(\text{CSR}_{7.5}) \quad (8)$$

In Equation 8,  $\text{CSR}$  is computed using the equation proposed by Seed et al. [44]. The  $N_{1,60CS}$  values were calculated using the corresponding clean-sand adjusted  $N$  values Youd et al. [37].

On the same database of 243 instances, Juang et al. [45] utilized the Bayesian mapping technique to estimate the liquefaction probability ( $P_L$ ) as a function of safety factor ( $F_s$ ). The factor of safety was calculated utilizing the SPT-based technique described in Youd et al. [41]. The following Equation 9 illustrates this:

$$P_L = \frac{1}{1 + \left[ \frac{F_s}{A} \right]^B} \quad (9)$$

In Equation 9, the regression coefficients  $A = 0.77$  and  $B = 3.25$ , Juang et al. [45] were used to determine the likelihood of liquefaction using the revised database of liquefaction case histories by Idriss and Boulanger [36, 46]. They used a variety of theories to construct different probability models, including the principles of Maximum Likelihood and Information Theory.

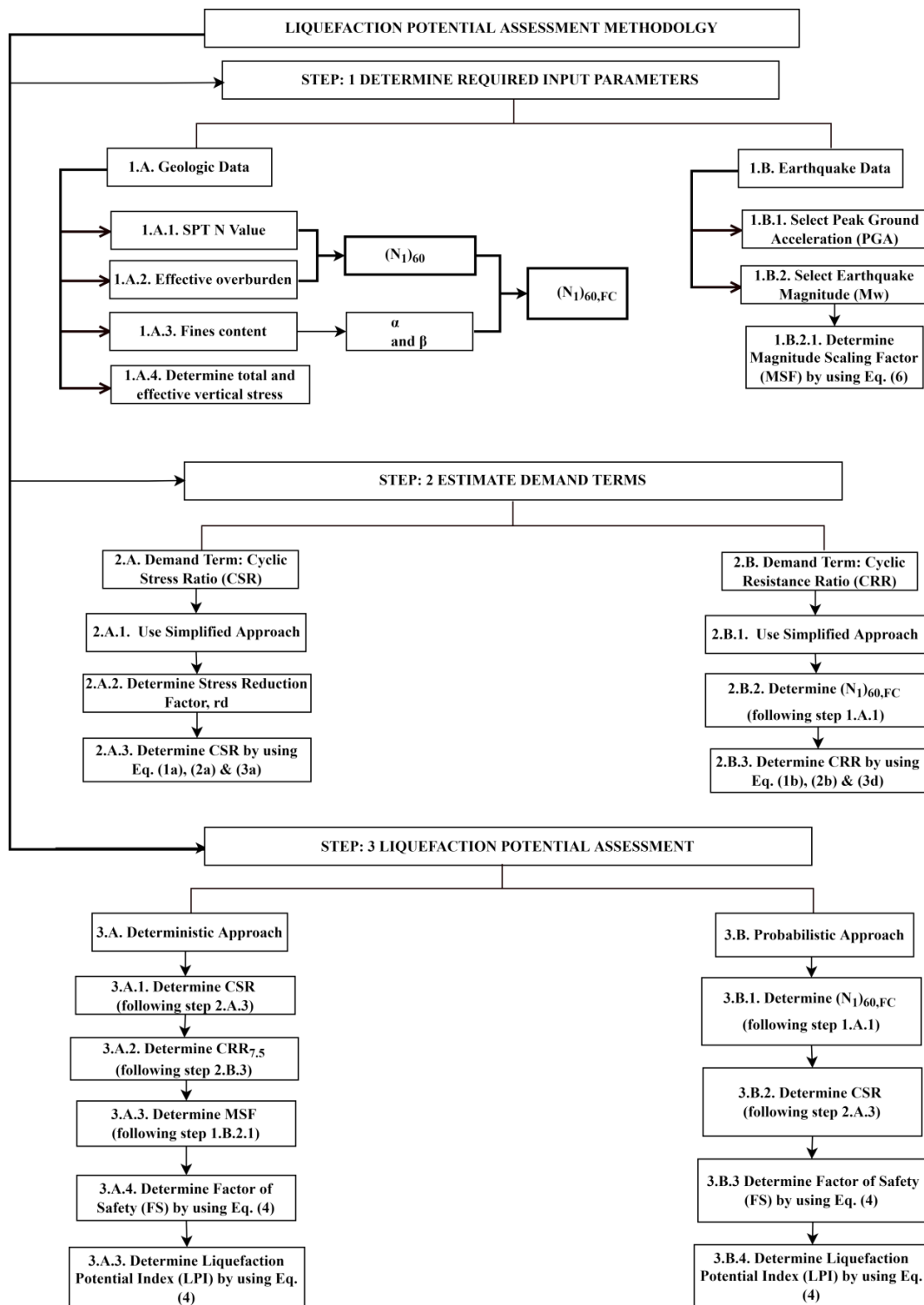


Figure 3. Liquefaction susceptibility evaluation methodology

According to them, the Gaussian + M1 model and the Logistic + M1 model performed well among the numerous models. The equation for the logistic+M1 model is as follows:

$$P_L = \frac{1}{1 + \exp[7.55(F_S - 0.95)]} \tag{10}$$

The liquefaction probability ( $P_L$ ) can be calculated as a function of cyclic stress ratio and cyclic resistance ratio, or as a function of the safety factor ( $F_S$ ). This  $P_L$ - $F_S$  mapping function is unique to the Idriss and Boulanger [36] method; thus, the safety factor ( $F_S$ ) must be calculated by the Idriss and Boulanger [36] method.

Though both models may be utilized to predict the liquefaction probability, they chose to adopt a mixed model that combines the Gaussian + M1 and Logistic + M1 models, as indicated in Equation 5.

$$P_L = \left[ 1 - \Phi \left( \frac{F_S - 0.95}{0.24} \right) + \frac{1}{1 + \exp(7.55(F_S - 0.95))} \right] \tag{11}$$

In Equation 11,  $\Phi$  stands for the standard normal cumulative distribution function and  $F_S$  must be evaluated utilizing the Idriss and Boulanger [36] method.

The chance of liquefaction was evaluated using a maximum likelihood method and an upgraded case history database, as per Boulanger and Idriss [47]. Here,  $CSR_{7.5}$  and  $N_{1,60CS}$  must be calculated from the deterministic liquefaction triggering correlation proposed by Idriss and Boulanger [36].

$$P_L[(N1)_{60CS}, CSR_{7.5}, \sigma'v=1atm] = \Phi \left[ - \frac{\left\{ \frac{(N1)_{60CS}}{14.1} \right\} + \left\{ \frac{(N1)_{60CS}}{126} \right\}^2 + \left\{ \frac{(N1)_{60CS}}{23.6} \right\}^3 + \left\{ \frac{(N1)_{60CS}}{25.4} \right\}^4 - 2.67 - \ln(CSR_{7.5})}{\sigma \ln(R)} \right] \tag{12-a}$$

After re-arrangement, the model created and suggested by Boulanger and Idriss [47] for practice may be represented as the equation given below, according to Juang et al. [45]:

$$P_L = 1 - \Phi \left[ \frac{\{\ln(F_S) + 0.13\}}{0.13} \right] \tag{12-b}$$

In Equation 12-b,  $F_S$  must be calculated by the Idriss and Boulanger [48] method.

### 4. Liquefaction Analysis of Northwest Region of Bangladesh

Dinajpur is in northern Bangladesh, between 25°10' and 26°04' north latitude and 88°23' and 89°18' east longitude. The topography of the area is generally flat, with a slight southerly slope toward which important rivers like the Dhepa, Punarbhava, and Atrai flow. Since Dinajpur lies in the Terai basin, the soil is sandy, with a significantly higher sand-to-silt ratio than clay. Because of the presence of several fault lines, this area is extremely vulnerable to earthquakes (Bogra fault, Tripura fault, Sub Dauki fault, Shillong fault, and Assam fault). Figure 4 depicts a map of the Dinajpur district. It has 13 upazilas: Kaharole, Khansama, Ghoraghat, Chirirbandar, DinajpurSadar, Nawabganj, Parbatipur, Fulbari, Biral, Birampur, Bochaganj, and Hakimpur . Birganj is the largest upazila in Dinajpur's 13-upazila district.

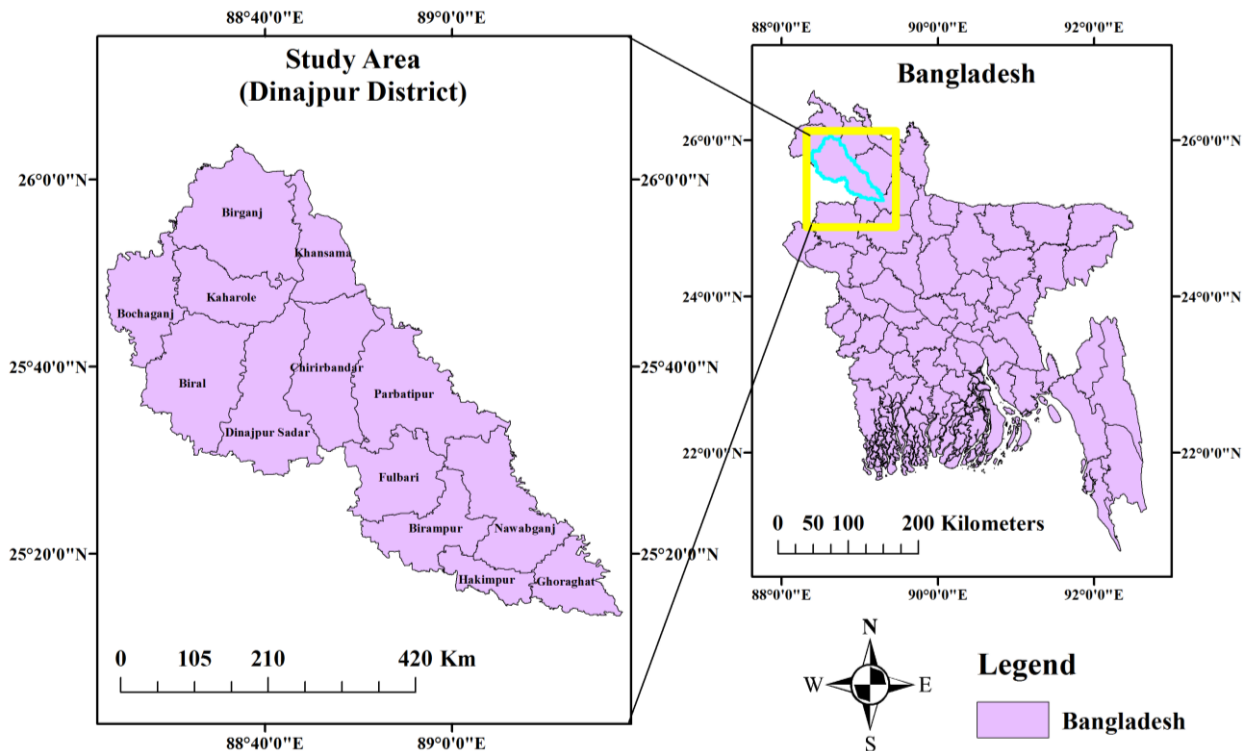
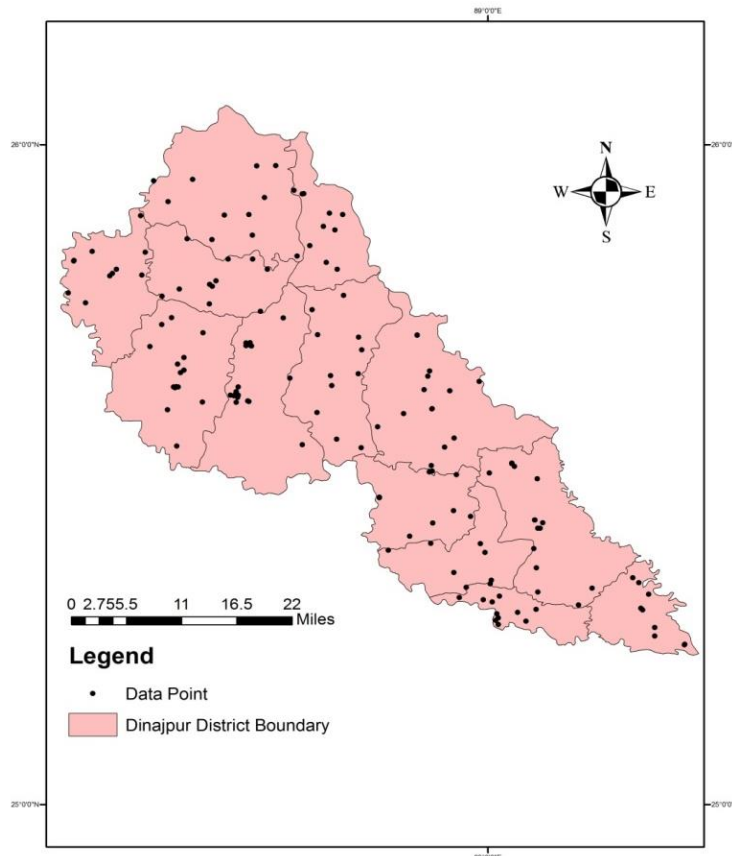


Figure 4. Map of Dinajpur district

Dinajpur District is quickly developing as a result of industrialization and urbanization. Many infrastructures are being constructed to satisfy the rising demand. As a result, subsoil investigations have been carried out at a number of places in all parts of the city. The current research collected geotechnical test reports from a variety of government and commercial institutions. A total of 160 soil test reports were obtained from various organizations and the essential data was retrieved from the soil test reports. The gathered sets of data can cover the majority of the region. Figure 5 shows the position of the boreholes.





**Figure 5. Borehole point locations in dinajpur district**

To calculate the cyclic stress ratio, effective and total overburden pressure was computed utilizing borehole data. In addition, the cyclic resistance ratio was calculated using SPT and  $N$  at various layers. Using the deterministic techniques mentioned above, the liquefaction factor of safety was determined. After that, the smoothing function was used to add the FS values together to get the LPI for the entire stratum. It is important to determine the liquefaction susceptibility of the entire stratum rather than FS at separate strata to measure the liquefaction susceptibility. As a result, LPI values are utilized to describe the extent of liquefaction in a given area. Using probabilistic approaches, the probability of liquefaction was also estimated. Following that, liquefaction severity is discussed using PL values. For the computation of the cyclic stress ratio, which is the produced stress in liquefaction a predicted earthquake magnitude and peak ground acceleration are required. The likelihood of a magnitude  $M_w = 7.0$  or greater earthquake in or around Bangladesh, specifically close to the Dinajpur district, is justified by the history of increasing earthquakes as well as the current frequency of seismic circulation. A magnitude 7.0 or larger earthquake is also possible, according to the suggested Bangladesh National Code (BNBC-2015).

Technical explanation is also required for an approximation of PGA. Dinajpur is positioned in seismic zone II, with a zone coefficient of 0.15, according to the previous BNBC-1993 seismic zonation map of Bangladesh, resulting in 0.15g peak ground acceleration. In recommended BNBC-2015, the existing seismic zonation map is updated to account for maximum anticipated earthquake motion in various parts of the country. According to the most recent BNBC-2015 seismic zonation map, Dinajpur lies in seismic zone II and has a zone coefficient of 0.2 and a probable PGA of 0.2g. Proposed PGA value is higher than the previous coefficient, making the zone very vulnerable to earthquakes. Following the preceding discussion, the revised BNBC-2015 guideline proposes using the magnitude and peak ground acceleration values of 6.5 and 0.20g, respectively, for earthquakes.

## 5. Results and Discussions

In the present research, the liquefaction safety factor, liquefaction potential index, and liquefaction probability were evaluated using data from 160 sites in the Dinajpur district. Liquefaction susceptibility was estimated using parameters for instance, the existence of sandy soil at a level of less than 20 m, shallow GWT (less than 10 m), and SPT- $N$  collected from the borehole report. The soil of Dinajpur is primarily alluvial, with a significantly larger proportion of sand and silt than clay. According to the 160 boring logs, the water level was 0–6 meters below the earth's surface.

Utilizing the three available deterministic methods mentioned above, the factor of safety (FS) for liquefaction was assessed for the study area. The safety factors (FS) for different layers of soil are assessed using an Mw 6.5 earthquake scenario with a PGA value of 0.20g. The factor of safety against liquefaction has been determined using the lowest safety factor among the estimated values. This safety factor may then be used to produce maps using Arc-GIS software that display the research area's safety factor hazards. Figure 6 shows the research region's FS mapping for 6.5 earthquake magnitudes at 3 meters of depth.

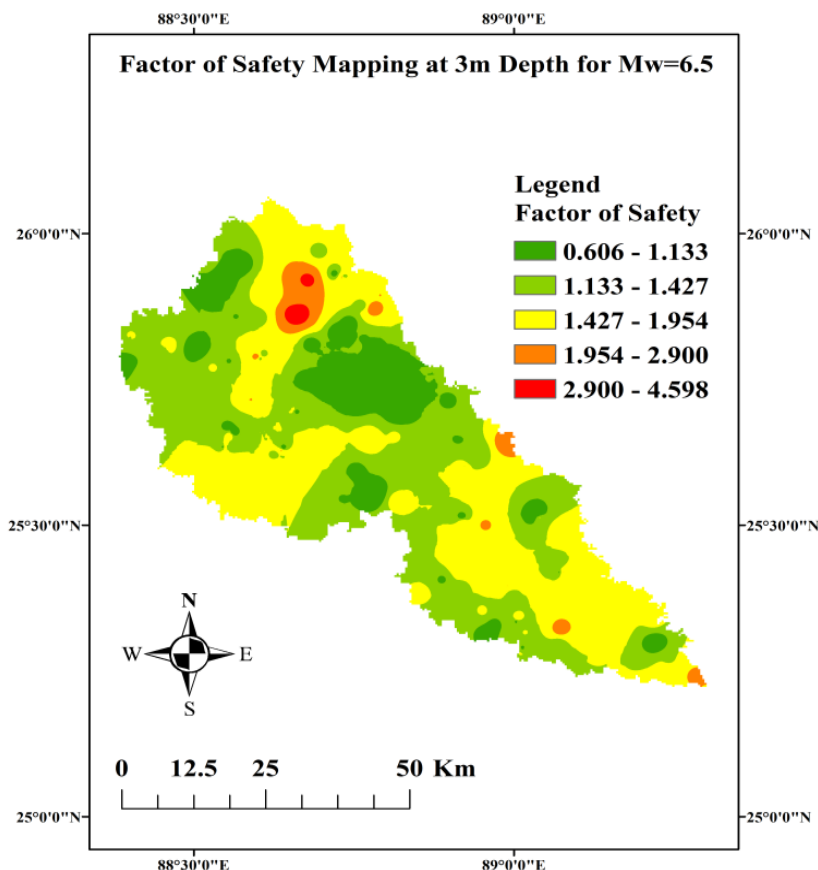


Figure 6. Borehole point locations in dinajpur district

About 35 of the 160 locations have FS values that are less than 1 and have been identified as liquefaction-prone. As shown by the image, the soils in the regions of Khansama, Chirirbandar, Dinajpur Sadar, Parbatipur, Bochaganj, and Biral were discovered to be liquefied with FS less than one. This may be due to the presence of filling land at shallow depths, followed by a layer of medium-sized sand that contains silt. The depth of the groundwater table below the surface is likewise shallow here.

Similar to this, the factor of safety for depths of 6 and 9 meters is also determined, and the danger map for each is shown in Figures 7 and 8, respectively. When taking into account the aforementioned magnitude, FS is determined to be less than 1 for 33 sites and 22 sites, respectively, at 6 m depth and 9 m depth, out of the 160 sites in the research regions. The risk map that was created also revealed that while certain areas in the South and Northwest are deemed to be securing from liquefaction, few places in the center of the map are. The location of the groundwater table in these certain places is at a greater depth. Due to the presence of clayey particles in the sand with SPT-N values of 25 and above, the majority of these locations display FS greater than 1.3-1.9.

The determined safety factor was then summed and weighed to establish the vulnerability of the layer, which is known as the LPI. According to Idriss and Boulanger (2006) [36] and Seed and Idriss (1971) [35], 36 locations had high liquefaction severity, whereas 35 sites had high liquefaction severity according to the Tokimatsu and Yoshimi (1983) [34] method of liquefaction analysis. On the other hand, according to Seed and Idriss (1971) [35], 7 locations had extremely high liquefaction severity. Figures 9-a to 9-e shows a comparison of LPI values for arbitrarily selected boreholes using the three different methods for different earthquake magnitudes.

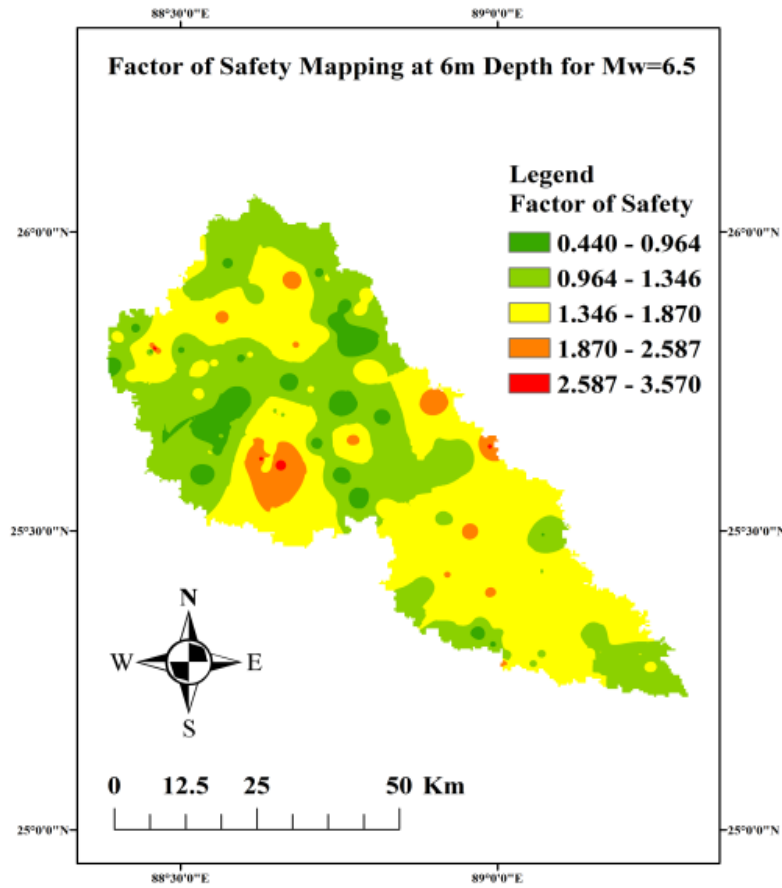


Figure 7. Borehole point locations in dinajpur district

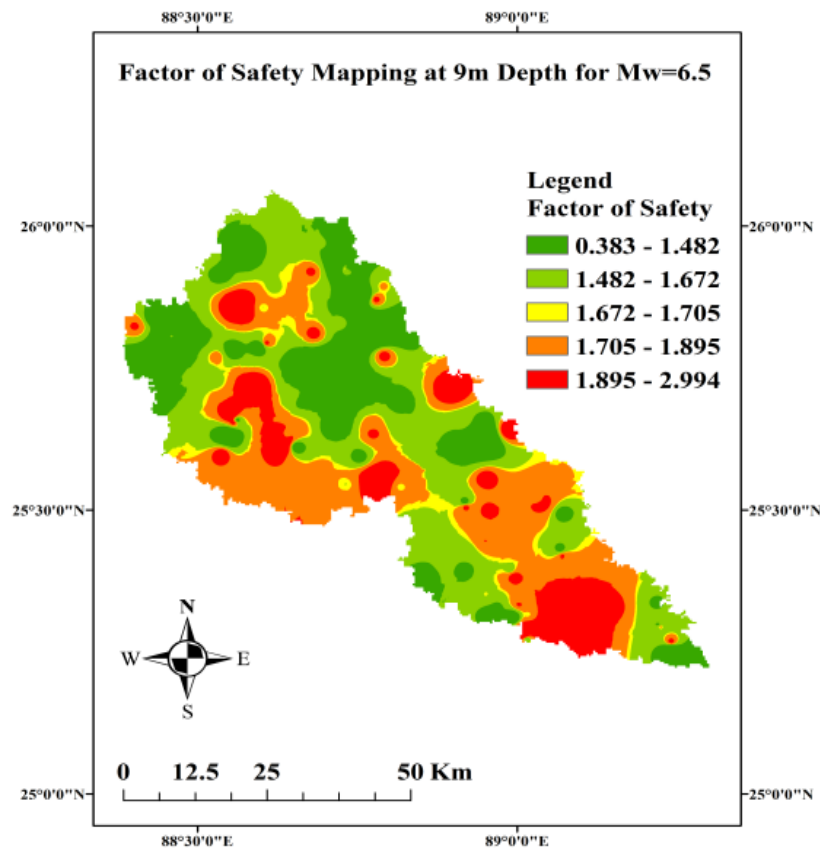


Figure 8. Borehole point locations in Dinajpur district

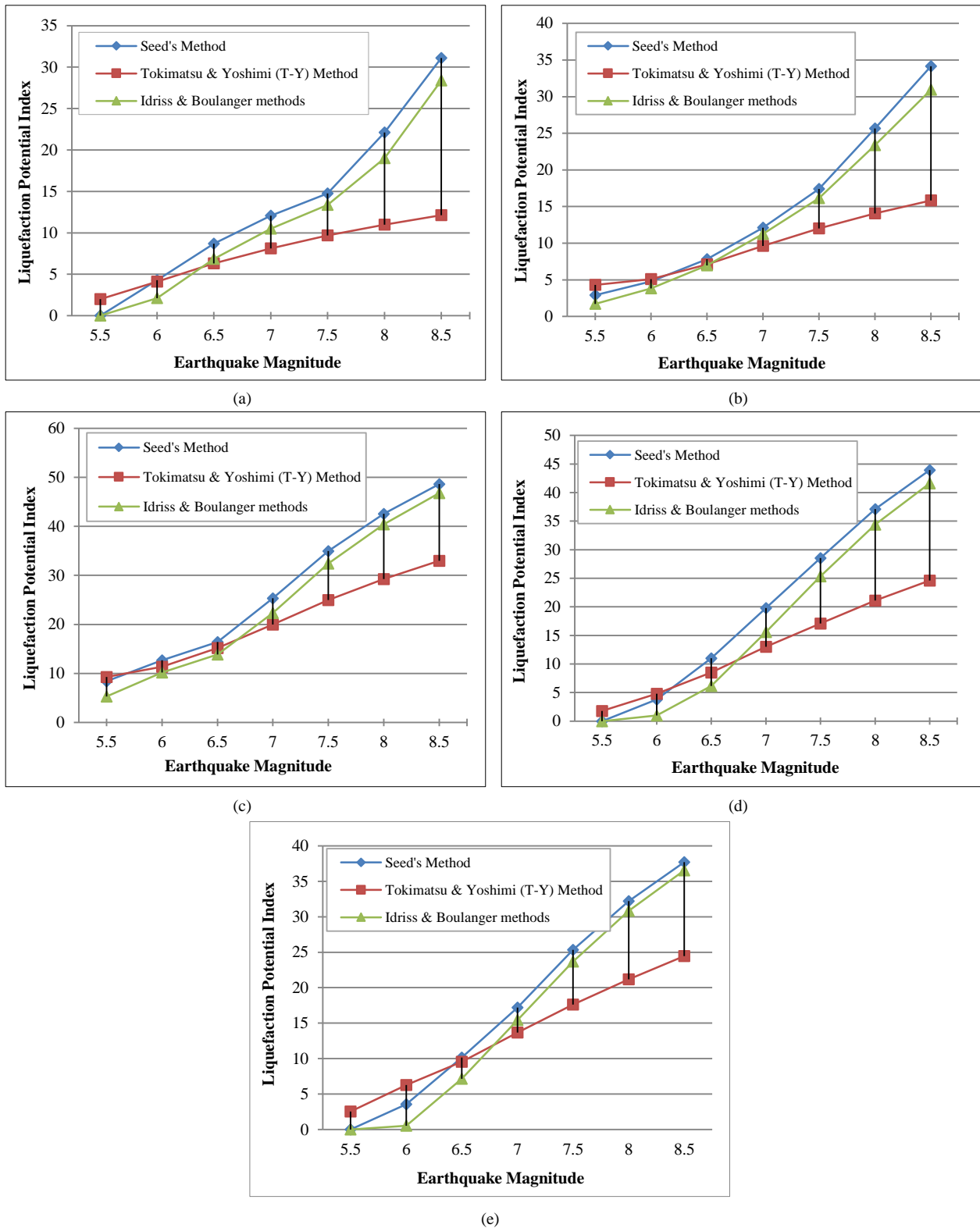
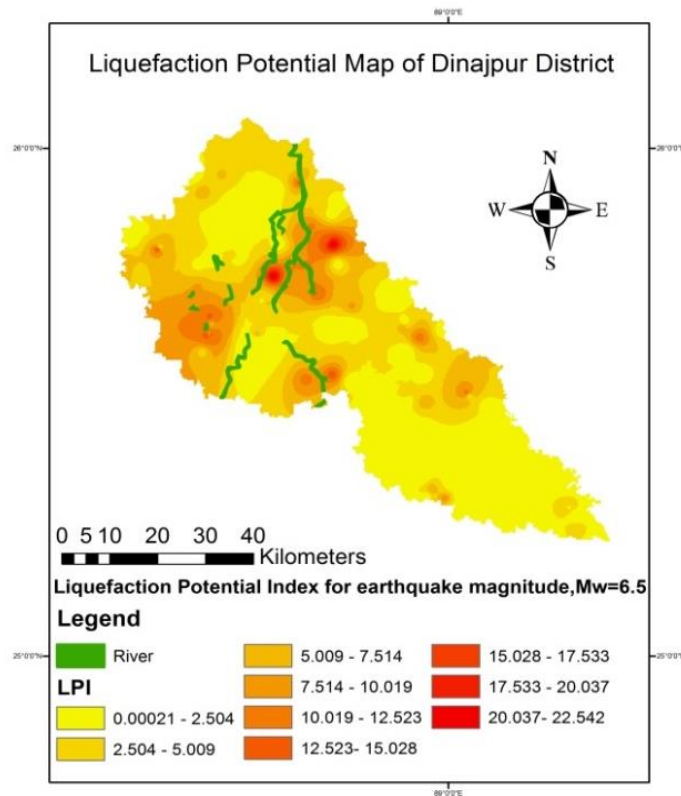


Figure 9. (a) LPI Comparison for bore 16 (b) LPI Comparison for bore 5 (c) LPI Comparison for bore 10 (d) LPI Comparison for bore 19 (e) LPI Comparison for bore 30

The pattern of variability is consistent across all graphs. The Seed and Idriss (1971) [35] technique yielded higher LPI values, while the Tokimatsu and Yoshimi (1983) [34] approach yielded lower LPI values, and the Idriss and Boulanger (2006) [36] method yielded LPI values in the middle of the two. On the other hand, the Tokimatsu and Yoshimi (1983) [34] technique, produces greater LPI values at smaller earthquake magnitudes. However, these discrete results do not represent the entire district's scenario. As a result, geospatial analysis (particularly IDW interpolation) was employed to represent the concentration of liquefaction vulnerability and probability of liquefaction over the study area in order to fulfill the demand. In the studied region, LPI calculations for 6.5 magnitude earthquakes ranged from 0 to 23, with very low and very high liquefaction danger (Figure 10). When the LPI score surpasses 15.0, the severity of liquefaction is very high. To better explain liquefaction phenomena, the legends display additional color bars.



**Figure 10. Liquefaction hazard map of Dinajpur district (Seed method) by IDW interpolation**

The majority of the region is “low liquefiable,” with the exception of a tiny part that is “high liquefiable,” according to LPI definitions. Furthermore, with the exception of a tiny portion of land that is "marginally liquefiable," the majority of the region is "non-liquefiable" ( $FS > 1.2$ ) according to factor of safety definitions. According to the Idriss and Boulanger (2006) [36] technique, LPI values for earthquake Mw= 6.5 ranged from 0 to 19, as shown in Figure 11.

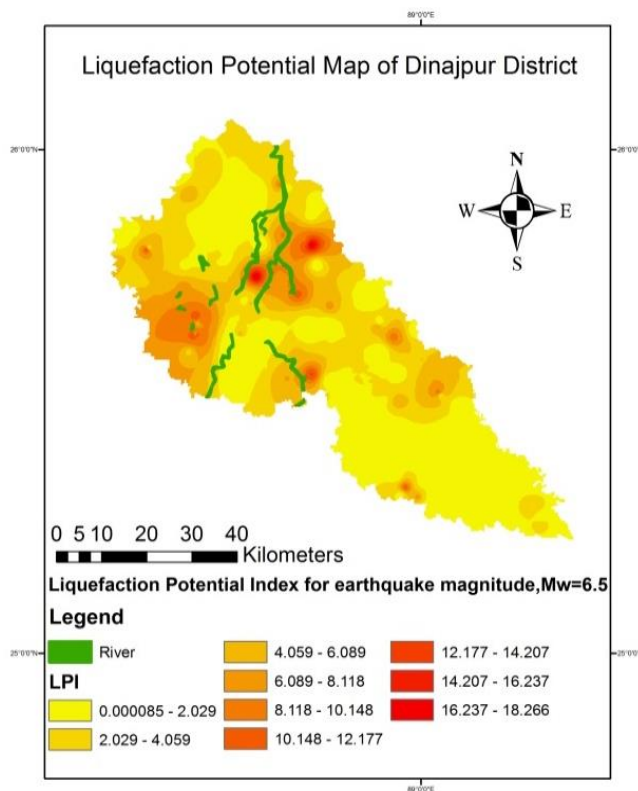


**Figure 11. Liquefaction hazard map of Dinajpur district (Idriss and Boulanger method) by IDW interpolation**

With the exception of a tiny portion of the research zone, the LPI value ranges from 5 to 15, as shown by the legend bar. The rest of the section shows LPI values from 0 to 5, as well as LPI > 15. The variation in LPI values was displayed by different colors. The majority of the region is “low liquefiable,” with the exception of a tiny part that is “high liquefiable,” according to LPI criteria. Figure 12 shows LPI values ranging from 0 to 20 according to the Tokimatsu and Yoshimi (1983) [34] technique.

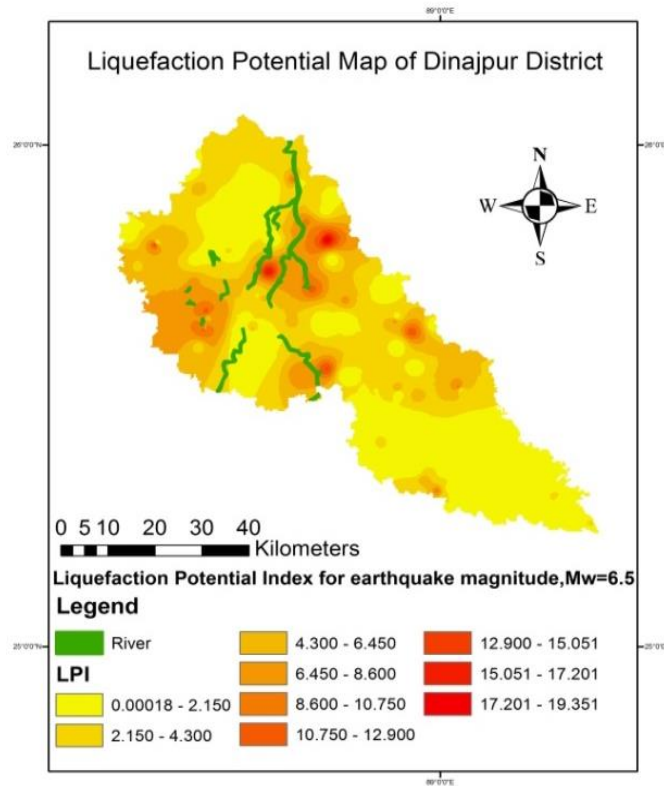
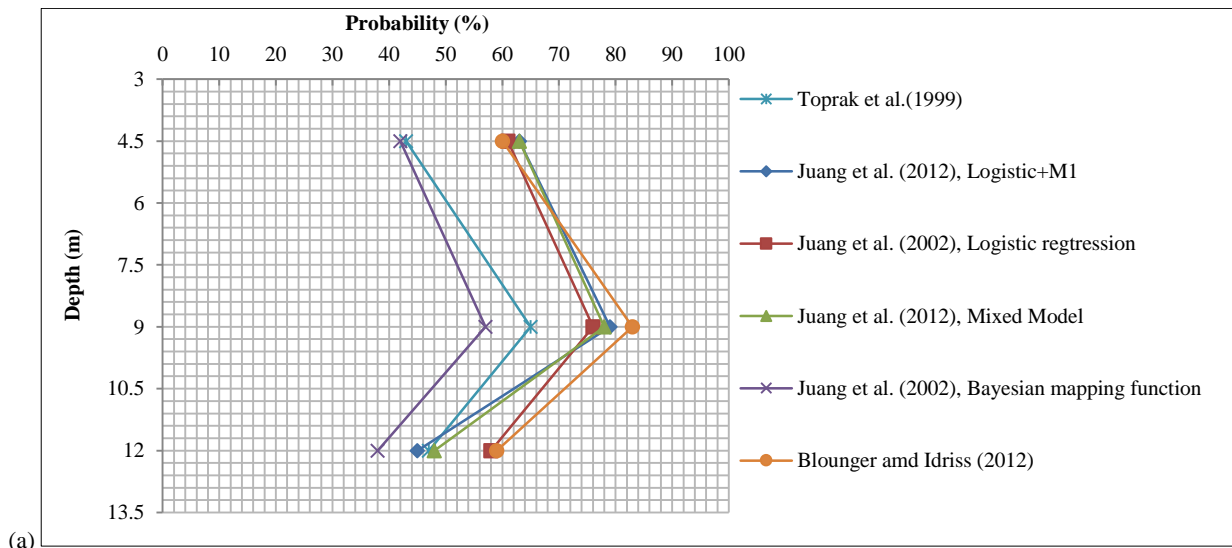


Figure 12. Liquefaction hazard map of Dinajpur district (Tokimatsu and Yoshimi Method) by IDW interpolation

The district's southern portion has been judged to be more resistant to liquefaction, while the district's center and northwestern sections have been determined to be more susceptible. With high LPI values, Upazila Biral, Birganj, Khansama, Parbatipur, and portions of Dinajpursadar are particularly vulnerable.

The six probabilistic techniques listed above were used to assess the probability of liquefaction. Out of 160 sites, 50 were identified to be vulnerable to liquefaction ( $P_L \geq 65\%$ ), according to Juang et al. (2002) [43], Logistic Regression and 49 sites, according to Juang et al. (2012) [45], Logistic+M1 and 51 sites, according to Juang et al. (2012) [45], Mixed model and 46 sites, according to Boulanger et al. (2012) [47]. Figures 13-a, and 13-b compares the liquefaction probability obtained using the six probabilistic techniques for arbitrarily selected boreholes in a liquefaction-prone soil layer for an earthquake of magnitude 6.5.



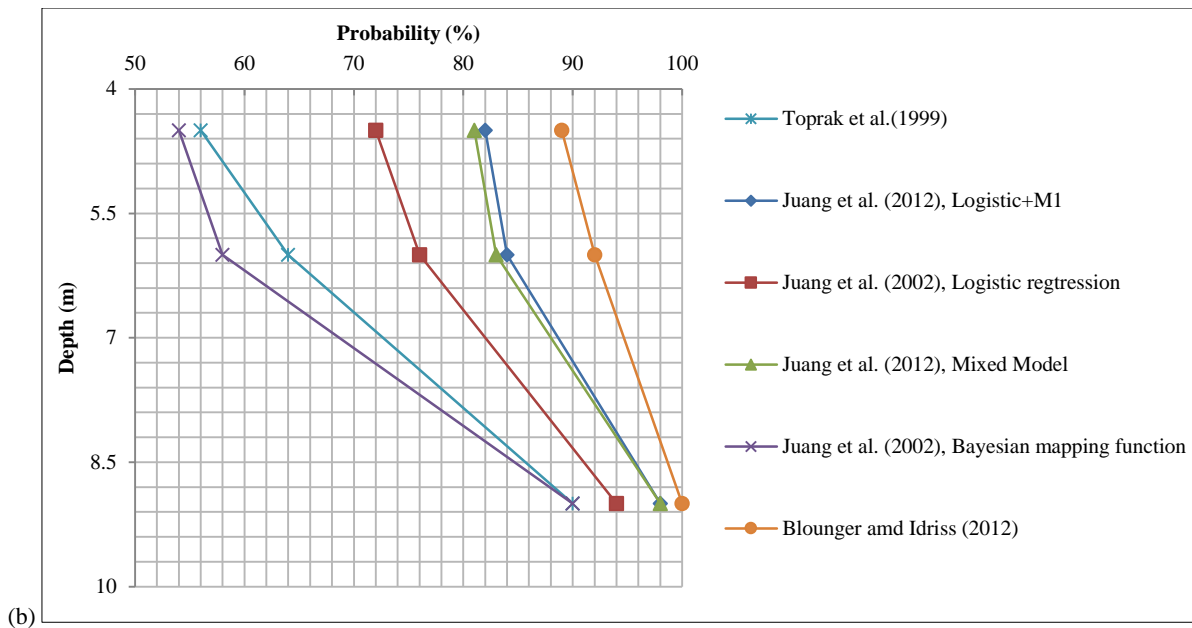


Figure 13. (a) Borehole 19 liquefaction probability comparison, (b) Borehole 33 liquefaction probability comparison

Boreholes 7, 16, 19, 26, 32, and 33 exhibit the same fluctuation pattern. Boulanger and Idriss (2012) [47], Juang et al. (2012) [45], Logistic+M1, Juang et al. (2012) [45], Mixed Model all come out with higher probability values. Juang et al. (2002) [43], the Bayesian mapping technique, and the Toprak et al. (1999) [42] Model all exhibit lower values. Juang et al. (2002) [43], Logistic Regression, provides probability values that are intermediate between Boulanger and Idriss (2012 [47]), Juang et al. (2012) [45], Logistic+M1, Juang et al. (2012) [45], Mixed Model, and Juang et al. (2002) [43], Bayesian mapping technique and Toprak et al. (1999) Model [42]. However, in a small number of boreholes, this pattern does not appear. The results obtained are consistent with those found previously [49].

According to Juang et al. (2002) [43], the PL-FS relationship is depicted in Figures 14-a, and 14-b, with probability computed using logistic regression analysis and the Bayesian mapping technique. In the Bayesian mapping technique, probability is proportional to the factor of safety. The expression of the equation differs in the logistic regression technique, but the trend is identical to that of the Bayesian mapping technique. The Mixed Models and logistic + M1, according to Juang et al. (2012) [43], can be used to determine liquefaction probability. The probability of liquefaction is shown as a function of the safety factor in both models. As a result, the probability versus factor of safety is shown as a smooth curve in Figures 15a and 15-b, and the results of both models coincide. The findings are in accordance with what has already been observed by Sharma et al. (2018) [49].

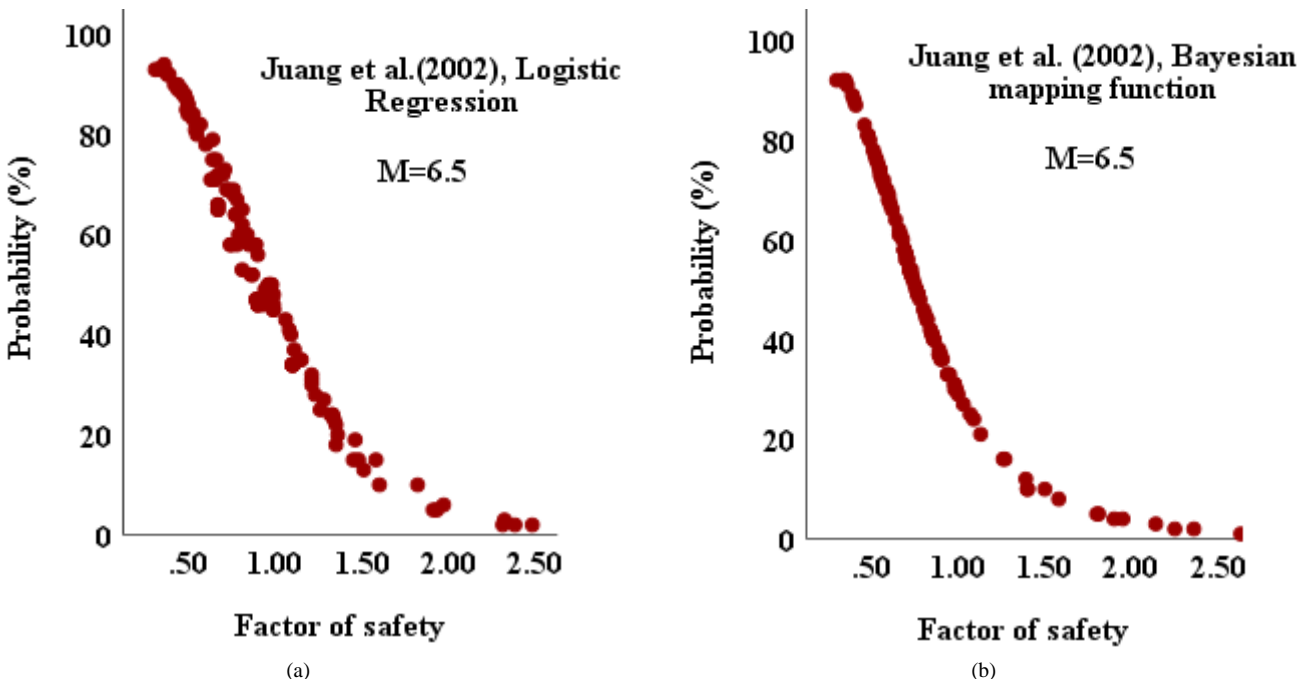


Figure 14. Relationship between probability and factor of safety evaluated by Juang et al. (2002)

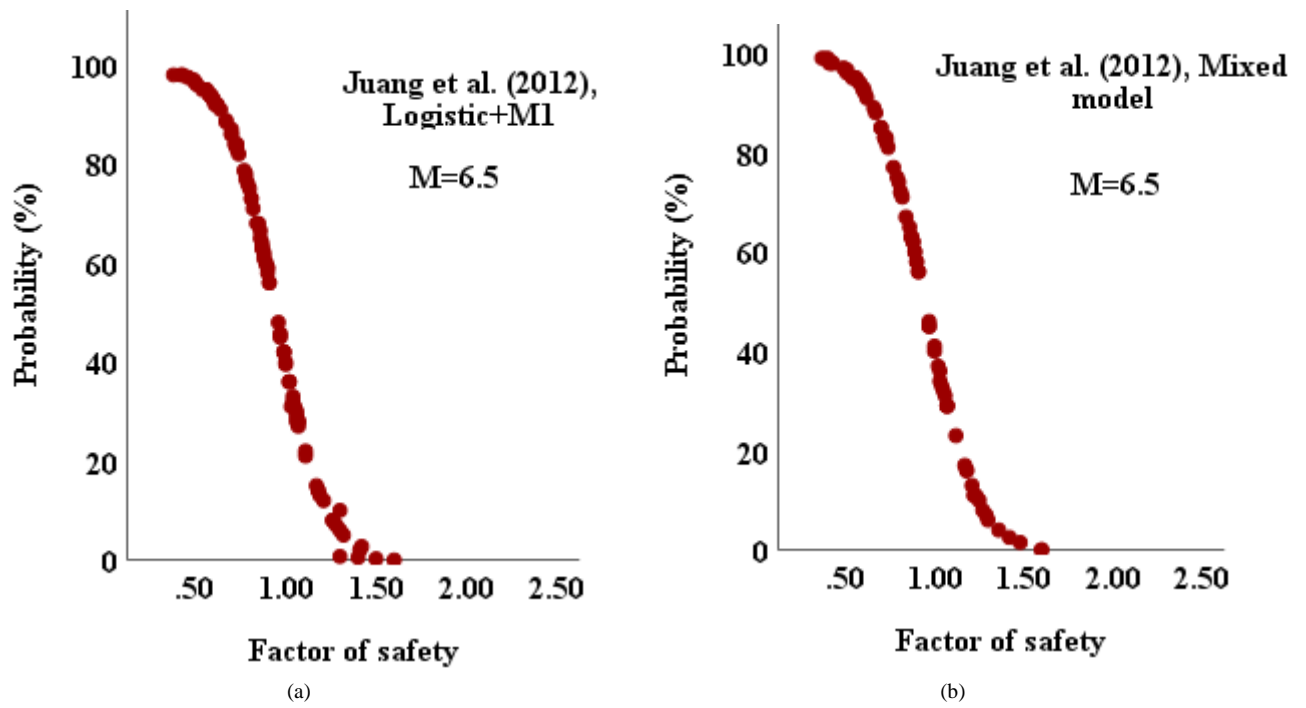
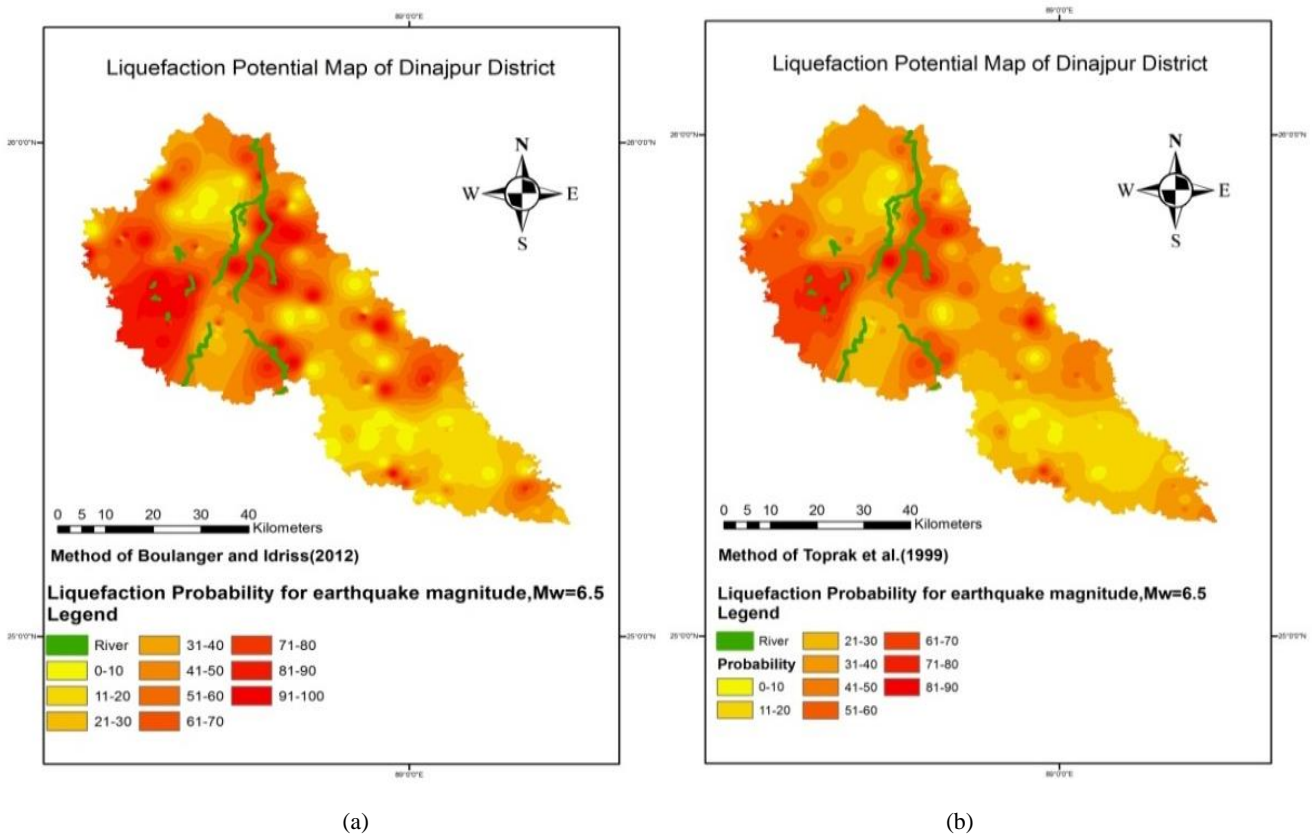
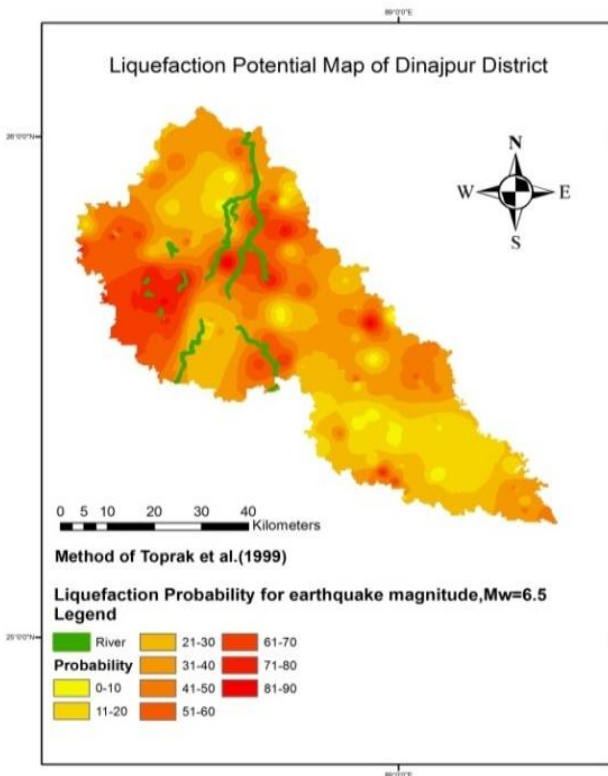


Figure 15. Relationship between probability evaluated by Juang et al. (2012) and factor of safety evaluated by Idriss and Boulanger (2004)

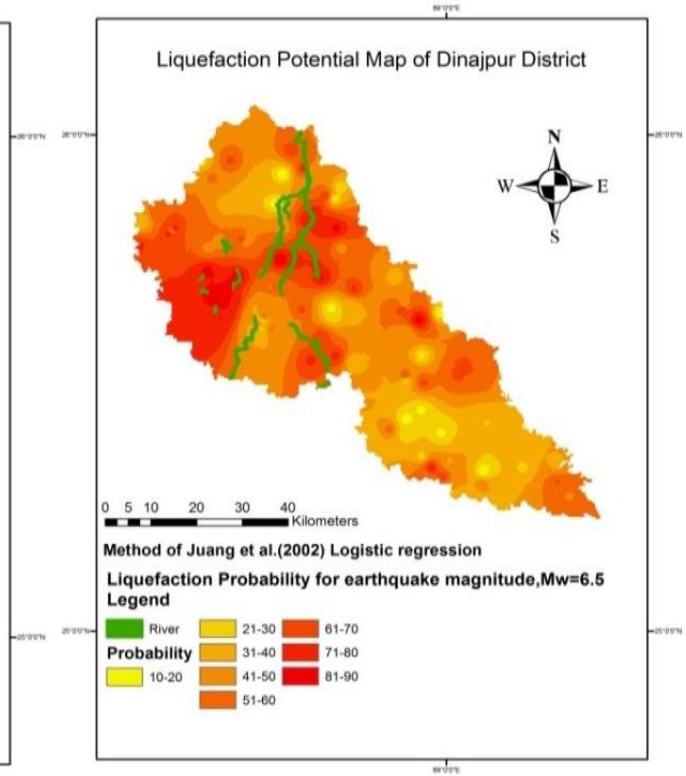
Figures 16-a to 16-f show the hazard map of Dinajpur district for a magnitude M=6.5 earthquake based on probabilistic methodologies by IDW interpolation. The stratum with the highest possibility of liquefaction is reserved as the liquefaction probability for that borehole when producing the hazard maps.



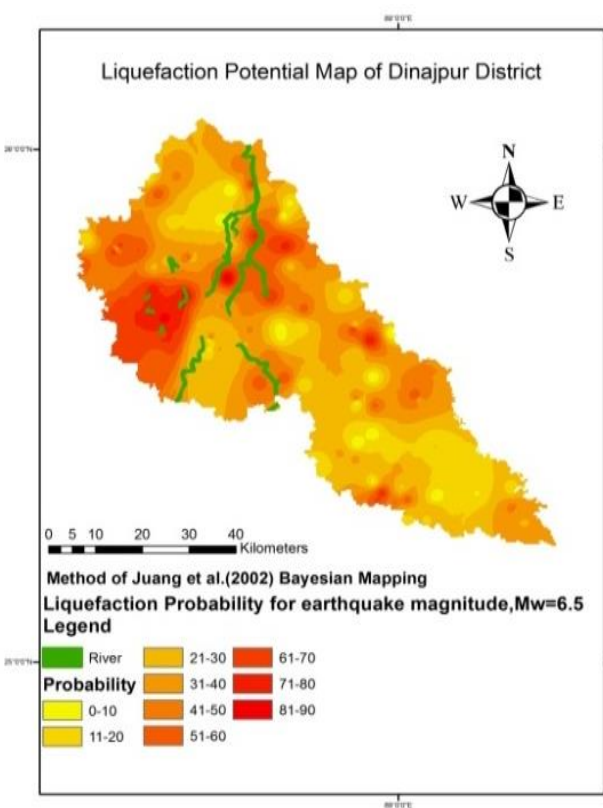




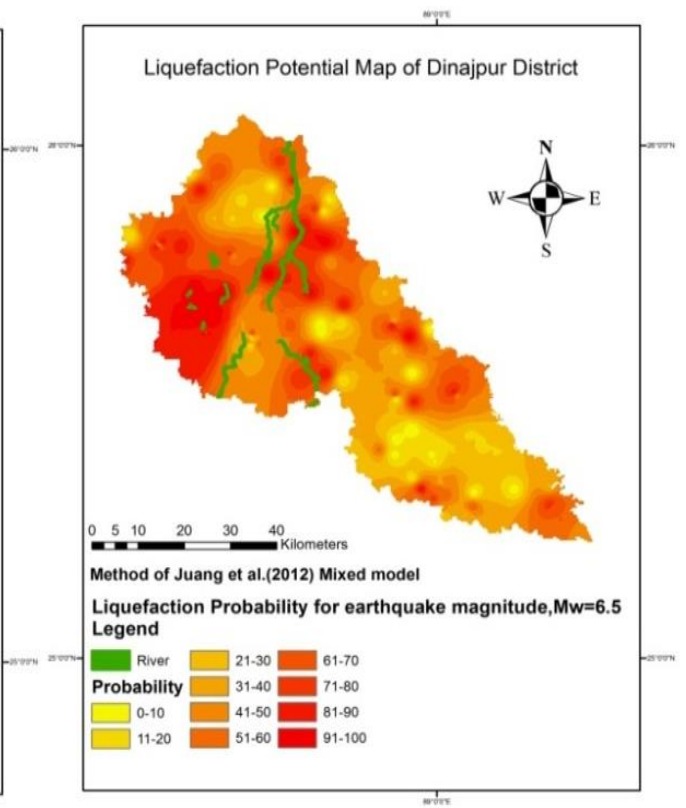
(c)



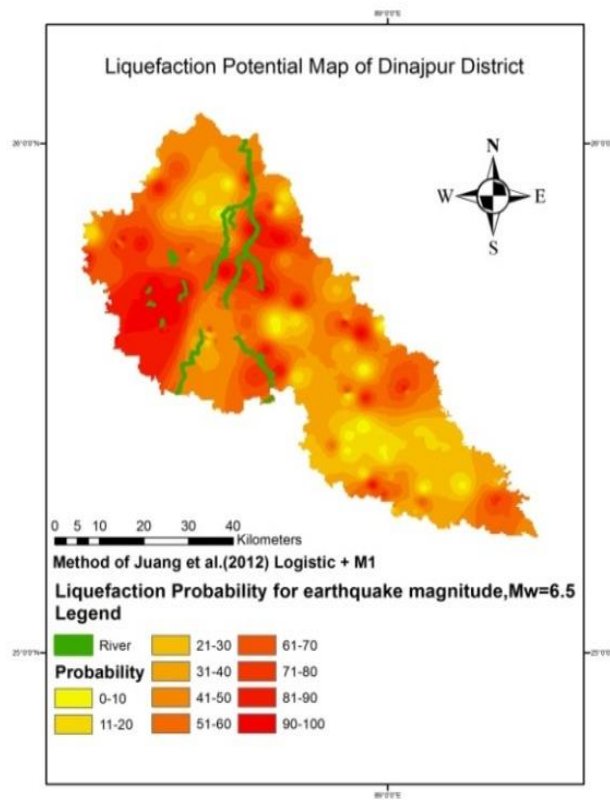
(d)



(e)



(f)



(f)

Figure 16. (a) Probabilistic liquefaction hazard map of Dinajpur District (Boulanger and Idriss 2012[47]) by IDW interpolation (b) Probabilistic liquefaction hazard map of Dinajpur District (Toprak et al. 1999 42) by IDW interpolation (c) Probabilistic liquefaction hazard map of Dinajpur District (method of Juang et al. (2002) Bayesian Mapping) by IDW interpolation (d) Probabilistic liquefaction hazard map of Dinajpur District (method of Juang et al. (2012) [45] Mixed Model) by IDW interpolation (e) Probabilistic liquefaction hazard map of Dinajpur District (method of Juang et al. (2012) [45] Logistic + M1) by IDW interpolation.

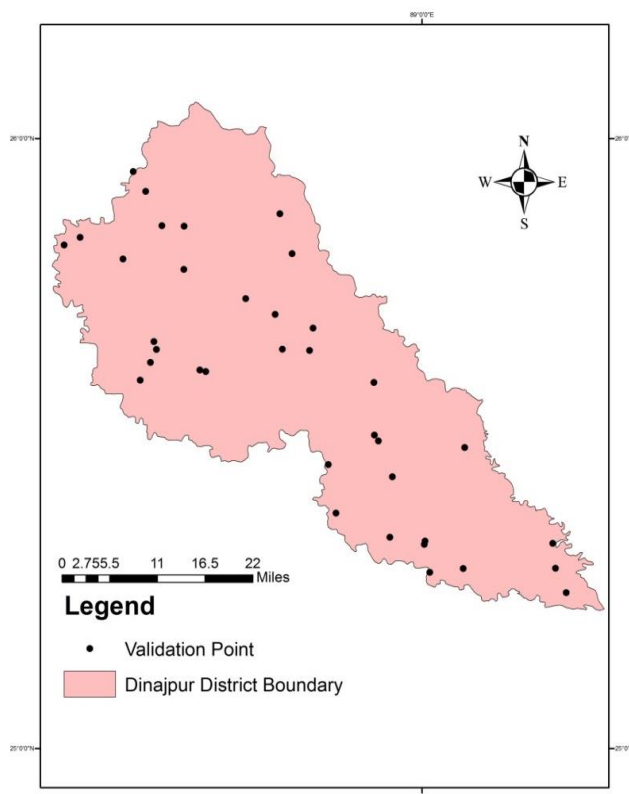


Figure 17. Second set of data used for validation of developed procedure

After that the Probability of liquefaction of the validation points were extracted from the hazard map. Regression analysis was conducted using the secondary data sets, and the results are displayed in Figure 18.

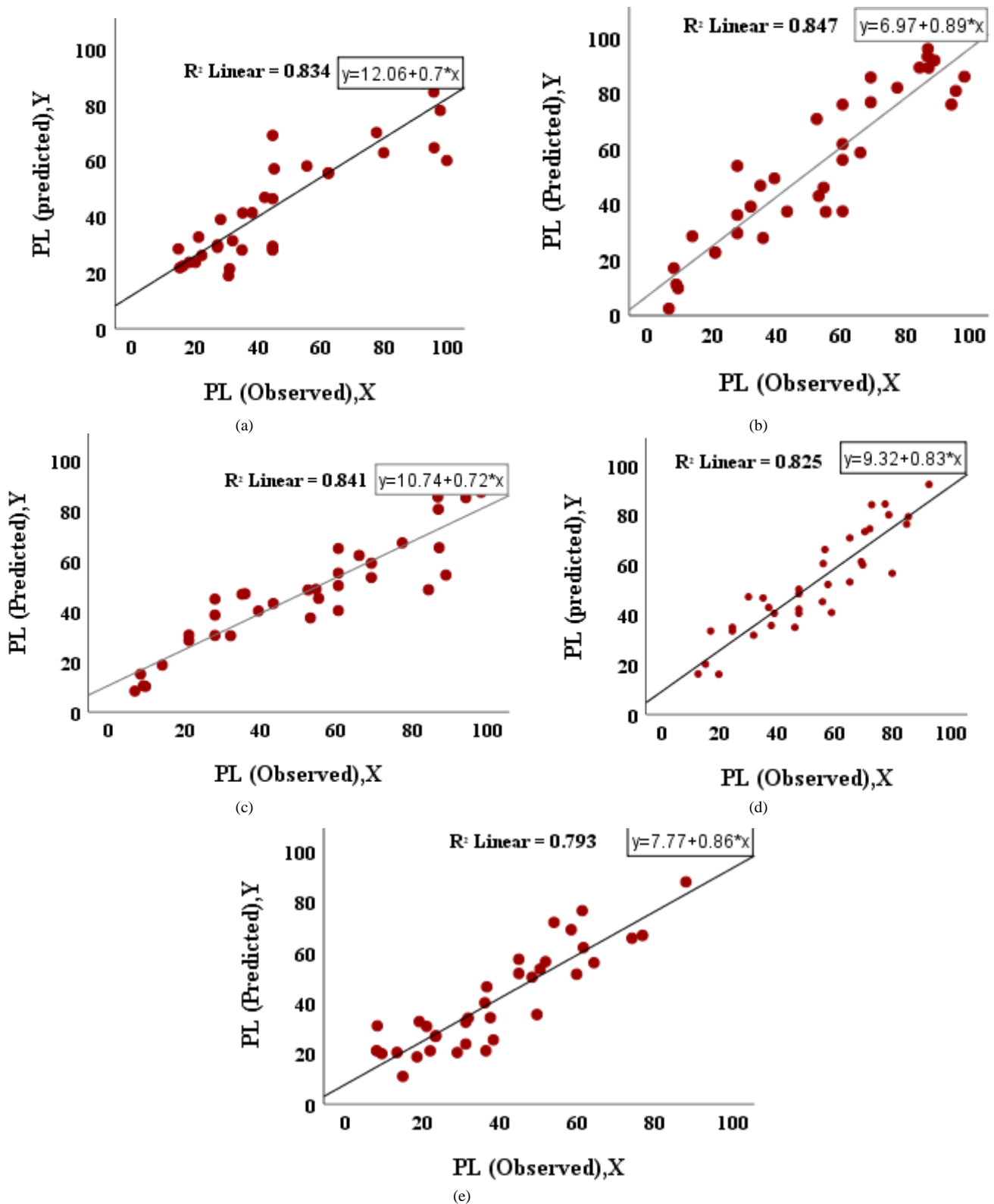


Figure 18. Observed and predicted probability of liquefaction (PL) values at validation points by IDW interpolation a) Method of Boulanger and Idriss (2012) [47] b) Method of Juang et al. (2012) [45] Logistic + M1 c) Method of Juang et al. (2012) [45] Mixed Model d) Method of Juang et al. (2002) [45] Bayesian Mapping.

In these figures, observed probability is plotted on the horizontal axis and probability from the prepared map is plotted on the vertical axis. The linear relationship between observed and predicted values has an R<sup>2</sup> value greater than 0.79 in all cases. The larger regression coefficient was seen for Juang et al. (2012) [45], Logistic+M1. The extracted value shows good consistency for the empirical methods.

## 6. Conclusions

This study mainly aims to attract interest in the present situation of liquefaction severity in Dinajpur district caused by seismic motion. The analysis is based on simplified deterministic and probabilistic methods using standard penetration test borehole data. Conventional approaches for assessing seismic soil liquefaction possibilities focus solely on a single value of peak ground acceleration and a single magnitude of earthquake. Based on the presence of sandy stratum up to a maximum of 20 meters, GWT at low depth (below 7m), and lower N-value (3–35), the city's vulnerability to liquefaction has been assessed. The findings are assessed in terms of soil liquefaction safety factor, liquefaction potential index, and liquefaction probability. Due to uncertainties in the liquefaction evaluation procedure, the results of this research were finally represented as seismic hazard maps, which show the study region's susceptible zones. Based on the outcomes, the following conclusion may be drawn:

- Out of 160 locations, deterministic processes revealed that 36 sites, including Kaharole (01), Khansama (03), Chirirbandar (05), Dinajpur Sadar (05), Nawabganj (01), Parbatipur (03), Fulbari (02), Biral (08), Birampur (01), Birganj (02), Bochaganj (04), and Hakimpur (01) had high liquefaction severity.
- According to probabilistic approaches, it has been determined that 50 sites, including Kaharole (03), Khansama (03), Chirirbandar (07), Dinajpur Sadar (06), Nawabganj (02), Parbatipur (03), Fulbari (03), Biral (10), Birampur (03), Birganj (02), Bochaganj (06), and Hakimpur (02), are likely to liquefy.
- For the research region, the adjusted N value necessary to prevent liquefaction ranges from 13 to 16 at depths of 3 m to 16 to 19 at depths of 6 m.
- The relationships between the probability of liquefaction and the factor of safety (FOS) obtained in this study are supported by, Juang et al. (2001) [43] and Sharma et al. (2018) [49].
- Since all possible combinations of ground accelerations and earthquake magnitudes were not considered in this study for the estimation of liquefaction potential, uncertainty in seismic loading wasn't taken into account.
- The derived hazard maps developed by probabilistic approaches were further validated to check the developed procedure using an arbitrarily collected secondary dataset. In every regression analysis event, the obtained  $R^2$  values exceeded 0.79. As a result, the created hazard maps for liquefaction susceptibility were justified by the greater regression coefficient. This produced hazard map may be utilized successfully for the Dinajpur district's planning, mitigation, and sustainable development.

## 7. Declarations

### 7.1. Author Contributions

Conceptualization, M.B.H., M.R. and M.M.R.; methodology, M.B.H.; formal analysis, M.B.H. and M.M.R.; data curation, M.R. and M.M.R.; writing—original draft preparation, M.B.H.; writing—review and editing, M.B.H., M.R. and M.M.R.; visualization, X.X.; supervision, M.R.; funding acquisition, M.B.H. and M.R. All authors have read and agreed to the published version of the manuscript.

### 7.2. Data Availability Statement

The data presented in this study are available on request from the corresponding author.

### 7.3. Funding

The authors received no financial support for the research, authorship, and/or publication of this article.

### 7.4. Acknowledgements

In Dinajpur, Bangladesh, the LGED, the PWD, the EED, and many private firms contributed critical data for this study. Throughout this investigation, the researcher would like to thank everybody who has provided them with ideas and information.

### 7.5. Conflicts of Interest

The authors declare no conflict of interest.

## 8. References

- [1] Mahabub, M. S., Hossain, A. T. M. S., & Pahlowan, E. U. D. (2020). Assessment of Liquefaction Potential from Sirajganj to Kurigram Area, Bangladesh. *IOSR Journal of Mechanical and Civil Engineering*, 17(1), 31–43. doi:10.9790/1684-1701033143.
- [2] Morino, M., Maksud Kamal, A. S. M., Muslim, D., Ekram Ali, R. M., Kamal, M. A., Zillur Rahman, M., & Kaneko, F. (2011). Seismic event of the Dauki Fault in 16th century confirmed by trench investigation at Gabrakhari Village, Haluaghat, Mymensingh, Bangladesh. *Journal of Asian Earth Sciences*, 42(3), 492–498. doi:10.1016/j.jseaes.2011.05.002.

- [3] Morino, M., Kamal, A. S. M. M., Akhter, S. H., Rahman, M. Z., Ali, R. M. E., Talukder, A., ... Kaneko, F. (2014). A paleo-seismological study of the Dauki fault at Jaflong, Sylhet, Bangladesh: Historical seismic events and an attempted rupture segmentation model. *Journal of Asian Earth Sciences*, 91, 218–226. doi:10.1016/j.jseaes.2014.06.002.
- [4] Steckler, M. S., Mondal, D. R., Akhter, S. H., Seeber, L., Feng, L., Gale, J., Hill, E. M., & Howe, M. (2016). Locked and loading megathrust linked to active subduction beneath the Indo-Burman Ranges. *Nature Geoscience*, 9(8), 615–18. doi:10.1038/ngeo2760.
- [5] Adnan, M. S. G., Talchabhadel, R., Nakagawa, H., & Hall, J. W. (2020). The potential of tidal river management for flood alleviation in south western Bangladesh. *Science of the Total Environment*, 731, 138747. doi:10.1016/j.scitotenv.2020.138747.
- [6] Rahman, Z., & Siddiqua, S. (2016). Liquefaction resistance evaluation of soils using standard penetration test blow count and shear wave velocity. *Proceedings of the 69<sup>th</sup> Canadian geotechnical society*. Canadian Geotechnical Society, Vancouver, Canada.
- [7] Bilham, R., & England, P. (2001). Plateau “pop-up” in the great 1897 Assam earthquake. *Nature*, 410(6830), 806–809. doi:10.1038/35071057.
- [8] Hossain, B. (2021). Empirical Correlation between Shear Wave Velocity and Uncorrected Standard Penetration Resistance (SPT-N) for Dinajpur District, Bangladesh. *Journal of Nature, Science & Technology*, 1(3), 25–29. doi:10.36937/janset.2021.003.005.
- [9] Rahman, M. A., Ahmed, S., & Imam, M. O. (2020). Rational Way of Estimating Liquefaction Severity: An Implication for Chattogram, the Port City of Bangladesh. *Geotechnical and Geological Engineering*, 38(2), 2359–2375. doi:10.1007/s10706-019-01134-2.
- [10] Coduto, D. P. (1999). *Geotechnical engineering: principles and practices*. Pearson College Division, New York City, United States.
- [11] Papathanassiou, G., Seggis, K., & Pavlides, S. (2011). Evaluating earthquake-induced liquefaction in the urban area of Larissa, Greece. *Bulletin of Engineering Geology and the Environment*, 70(1), 79–88. doi:10.1007/s10064-010-0281-3.
- [12] Mihajlović, G., & Živković, M. (2020). Sieving Extremely Wet Earth Mass by Means of Oscillatory Transporting Platform. *Emerging Science Journal*, 4(3), 172–182. doi:10.28991/esj-2020-01221.
- [13] Peng, E., Hou, Z., Sheng, Y., Hu, X., Zhang, D., Song, L., & Chou, Y. (2021). Anti-liquefaction performance of partially saturated sand induced by biogas under high intensity vibration. *Journal of Cleaner Production*, 319, 128794. doi:10.1016/j.jclepro.2021.128794.
- [14] Seed, H. B., & Idriss, I. M. (1967). Analysis of Soil Liquefaction: Niigata Earthquake. In *Journal of the Soil Mechanics and Foundations Division*, 93(3), 83–108. doi:10.1061/jsfea.0000981.
- [15] Erdik, M. (2001). Report on 1999 Kocaeli and Duzce (Turkey) Earthquakes, Structural control for civil and infrastructure engineering. World Scientific, Singapore. doi:10.1142/9789812811707\_0018.
- [16] Bray, J. D., & Sancio, R. B. (2006). Assessment of the Liquefaction Susceptibility of Fine-Grained Soils. *Journal of Geotechnical and Geoenvironmental Engineering*, 132(9), 1165–1177. doi:10.1061/(ASCE)1090-0241(2006)132:9(1165).
- [17] Ansary, M. A., & Rashid, M. A. (2000). Generation of liquefaction potential map for Dhaka, Bangladesh. 8<sup>th</sup> ASCE Specialty Conference on Probabilistic Mechanics and Structural Reliability, 24-26 July, 2000, University of Notre Dame, Notre Dame, Indiana, United States.
- [18] Islam, M. S., & Hossain, M. T. (2010). Earthquake Induced Liquefaction Potential of Reclaimed Areas of Dhaka City. *GeoShanghai International Conference 2010*. doi:10.1061/41102(375)40.
- [19] Mhaske, S. Y., & Choudhury, D. (2010). GIS-based soil liquefaction susceptibility map of Mumbai city for earthquake events. *Journal of Applied Geophysics*, 70(3), 216–225. doi:10.1016/j.jappgeo.2010.01.001.
- [20] Thoithoi, L., Ningthoujam, P. S., Singh, R. P., & Shukla, D. P. (2013). Liquefaction Study of Subsurface Soil in Part of Delhi University, North Campus. *International Journal of Advancement in Earth and Environmental Science*, 1(1), 14–22.
- [21] Hossain, M. S., Kamal, A. S. M. M., Rahman, M. Z., Farazi, A. H., Mondal, D. R., Mahmud, T., & Ferdous, N. (2020). Assessment of soil liquefaction potential: a case study for Moulvibazar town, Sylhet, Bangladesh. *SN Applied Sciences*, 2(4). doi:10.1007/s42452-020-2582-x.
- [22] Sengupta, S., & Kolathayar, S. (2020). Evaluation of liquefaction potential of soil at a power plant site in Chittagong, Bangladesh. *International Journal of Geotechnical Earthquake Engineering*, 11(1), 1–16. doi:10.4018/IJGEE.2020010101.
- [23] Wadi, D., Wu, W., Malik, I., Ahmed, H. A., & Makki, A. (2021). Assessment of liquefaction potential of soil based on standard penetration test for the upper Benue region in Nigeria. In *Environmental Earth Sciences*, 80(7), 1-11. doi:10.1007/s12665-021-09565-y.
- [24] Abdullah, G. M. S., & El Aal, A. A. (2021). Liquefaction hazards mapping along Red Sea coast, Jeddah city, Kingdom of Saudi Arabia. *Soil Dynamics and Earthquake Engineering*, 144. doi:10.1016/j.soildyn.2021.106682.

- [25] Subedi, M., & Acharya, I. P. (2022). Liquefaction hazard assessment and ground failure probability analysis in the Kathmandu Valley of Nepal. *Geoenvironmental Disasters*, 9(1). doi:10.1186/s40677-021-00203-0.
- [26] Tint, Z. L., Kyaw, N. M., & Kyaw, K. (2018). Development of soil distribution and liquefaction potential maps for downtown area in Yangon, Myanmar. *Civil Engineering Journal*, 4(3), 689-701. doi:10.28991/cej-0309108.
- [27] Hossain, M. S., Xiao, W., Khan, M. S. H., Chowdhury, K. R., & Ao, S. (2020). Geodynamic model and tectono-structural framework of the Bengal Basin and its surroundings. *Journal of Maps*, 16(2), 445–458. doi:10.1080/17445647.2020.1770136
- [28] Hossain, M.S., Khan, M.S.H., Chowdhury, K.R., Abdullah, R. (2019). Synthesis of the Tectonic and Structural Elements of the Bengal Basin and Its Surroundings. *Tectonics and Structural Geology: Indian Context*. Springer Geology. Springer, Cham, Switzerland. doi:10.1007/978-3-319-99341-6\_6.
- [29] Khan, M. S. H., Hossain, M. S., & Chowdhury, K. R. (2017). Geomorphic Implications and active tectonics of the Sitapahar Anticline–CTFB, Bangladesh. *Bangladesh Geoscience Journal*, 23, 1–24.
- [30] Curray, J.R., Emmel, F.J., Moore, D.G., Raitt, R.W. (1982). Structure, Tectonics, and Geological History of the Northeastern Indian Ocean. *The Ocean Basins and Margins*. Springer, Boston, United States. doi:10.1007/978-1-4615-8038-6\_9.
- [31] Ambraseys, N. N., & Douglas, J. (2004). Magnitude calibration of north Indian earthquakes. *Geophysical Journal International*, 159(1), 165–206. doi:10.1111/j.1365-246X.2004.02323.x
- [32] Alam, M. K., Hasan, A. K. M., Khan, M. R., & Whitney, J. W. (1990). Geological Map of Bangladesh. Geological Survey of Bangladesh. US Geological Survey, Dhaka, Bangladesh.
- [33] Chang, M., Kuo, C. ping, Shau, S. hui, & Hsu, R. eeh. (2011). Comparison of SPT-N-based analysis methods in evaluation of liquefaction potential during the 1999 Chi-chi earthquake in Taiwan. *Computers and Geotechnics*, 38(3), 393–406. doi:10.1016/j.compgeo.2011.01.003.
- [34] Tokimatsu, K., & Yoshimi, Y. (1983). Empirical Correlation of Soil Liquefaction Based on SPT N-Value and Fines Content. *Soils and Foundations*, 23(4), 56–74. doi:10.3208/sandf1972.23.4\_56
- [35] Seed, H.B., & Idriss, I.M. (1971). Simplified procedure for evaluating soil liquefaction potential. *Journal of the Soil Mechanics and foundation Divisions*, 97(9), 1249–1273. doi:10.1061/jrseaq.0001662.
- [36] Idriss, I. M., & Boulanger, R. W. (2006). Semi-empirical procedures for evaluating liquefaction potential during earthquakes. *Soil Dynamics and Earthquake Engineering*, 26(2-4), 115–130. doi:10.1016/j.soildyn.2004.11.023
- [37] Youd, T. L., & Idriss, I. M. (1997). Proceeding of the NCEER workshop on evaluation of liquefaction resistance of soils. Report NCEER-97-0022, Brigham Young University, Provo, United States.
- [38] Rauch, A. F. (1997). An empirical method for predicting surface displacements due to liquefaction-induced lateral spreading in earthquakes. PhD Thesis, Virginia Tech, Blacksburg, United States.
- [39] Luna, R., & Frost, J. D. (1998). Spatial Liquefaction Analysis System. *Journal of Computing in Civil Engineering*, 12(1), 48–56. doi:10.1061/(asce)0887-3801(1998)12:1(48).
- [40] Iwasaki, T., Tokida, K. I., Tatsuoka, F., Watanabe, S., Yasuda, S., & Sato, H. (1982). Microzonation for soil liquefaction potential using simplified methods. *Proceedings of the 3<sup>rd</sup> International Conference on Microzonation*, 28 June-1 July, 1982, Seattle, United States.
- [41] Youd, T. L., & Idriss, I. M. (2001). Liquefaction Resistance of Soils: Summary Report from the 1996 NCEER and 1998 NCEER/NSF Workshops on Evaluation of Liquefaction Resistance of Soils. *Journal of Geotechnical and Geoenvironment Engineering*, 127(4), 297–313. doi:10.1061/(asce)1090-0241(2001)127:4(297).
- [42] Toprak, S., Holzer, T. L., Bennett, M. J., & Tinsley III, J. C. (1999). CPT-and SPT-based probabilistic assessment of liquefaction. 7<sup>th</sup> US–Japan Workshop on Earthquake Resistant Design of Lifeline Facilities and Countermeasures against Liquefaction, Multidisciplinary Center for Earthquake Engineering Research, 15-17 August, Seattle, United States.
- [43] Juang, C. H., Jiang, T., & Andrus, R. D. (2002). Assessing probability-based methods for liquefaction potential evaluation. *Journal of Geotechnical and Geoenvironmental Engineering*, 128(7), 580-589. doi:10.1061/(ASCE)1090-0241(2002)128:7(580).
- [44] Bolton Seed, H., Tokimatsu, K., Harder, L. F., & Chung, R. M. (1985). Influence of SPT procedures in soil liquefaction resistance evaluations. *Journal of Geotechnical Engineering*, 111(12), 1425–1445. doi:10.1061/(ASCE)0733-9410(1985)111:12(1425).
- [45] Juang, C. H., Ching, J., Luo, Z., & Ku, C. S. (2012). New models for probability of liquefaction using standard penetration tests based on an updated database of case histories. *Engineering Geology*, 133–134, 85–93. doi:10.1016/j.enggeo.2012.02.015.

- [46] Gowda, G. B., Dinesh, S. V., Govindaraju, L., & Babu, R. R. (2022). Effect of Liquefaction Induced Lateral Spreading on Seismic Performance of Pile Foundations. *Civil Engineering Journal*, 7, 58-70. doi:10.28991/CEJ-SP2021-07-05.
- [47] Boulanger, R. W., & Idriss, I. M. (2012). Probabilistic standard penetration test–based liquefaction–triggering procedure. *Journal of Geotechnical and Geoenvironmental Engineering*, 138(10), 1185-1195. doi:10.1061/(ASCE) GT.1943-5606.0000700.
- [48] Idriss, I. M., & Boulanger, R. W. (2010). Report on SPT-based liquefaction triggering procedures. Report number: UCD/CGM-10/02, Center for Geotechnical Modeling, Department of Civil and Environmental Engineering, University of California at Davis, Davis, United States.
- [49] Sharma, B., Siddique, A. F., Medhi, B. J., & Begum, N. (2018). Assessment of liquefaction potential of Guwahati city by probabilistic approaches. *Innovative Infrastructure Solutions*, 3(1), 1-12. doi:10.1007/s41062-017-0117-0.